

Efficient numerical valuation of European options under the two-asset Kou jump-diffusion model

Karel J. in 't Hout* and Pieter Lamotte*

March 20, 2023

Abstract

This paper concerns the numerical solution of the two-dimensional time-dependent partial integro-differential equation (PIDE) that holds for the values of European-style options under the two-asset Kou jump-diffusion model. A main feature of this equation is the presence of a nonlocal double integral term. For its numerical evaluation, we extend a highly efficient algorithm derived by Toivanen [36] in the case of the one-dimensional Kou integral. The acquired algorithm for the two-dimensional Kou integral has optimal computational cost: the number of basic arithmetic operations is directly proportional to the number of spatial grid points in the semidiscretization. For the effective discretization in time, we study seven contemporary operator splitting schemes of the implicit-explicit (IMEX) and the alternating direction implicit (ADI) kind. All these schemes allow for a convenient, explicit treatment of the integral term. We analyze their (von Neumann) stability. By ample numerical experiments for put-on-the-average option values, the actual convergence behavior as well as the mutual performance of the seven operator splitting schemes are investigated. Moreover, the Greeks Delta and Gamma are considered.

Keywords: partial integro-differential equations, operator splitting methods, implicit-explicit schemes, alternating direction implicit schemes, stability, convergence, Kou model, European options.

1 Introduction

In contemporary financial option valuation theory, jump-diffusion processes form a principal class of models for the evolution of the underlying asset prices, see e.g. Cont & Tankov [7] and Schoutens [34]. The first jump-diffusion process was proposed in 1976 by Merton [29]. In this classical model, the relative jump sizes are assumed to be lognormally distributed. A wide variety of jump-diffusion processes, and more generally, exponential Lévy processes, for asset prices has been introduced in the literature since then, for example the familiar variance gamma (VG), normal inverse Gaussian (NIG) and Carr–Geman–Madan–Yor (CGMY) models [7, 34].

In this paper we consider the jump-diffusion model proposed by Kou [27]. In this model, the relative jump sizes are given by a log-double-exponential distribution. Just like the models mentioned above, Kou's jump-diffusion model has become popular in financial option valuation theory and practice. In this paper we are interested in the valuation of European-style options under a direct extension of Kou's single asset jump-diffusion model [27] to two assets. Here the finite activity jumps in the two asset prices are assumed to occur contemporaneously. Financial option valuation theory then yields a two-dimensional time-dependent partial integro-differential equation (PIDE) that must be satisfied for the values of European two-asset options. The integral part, which stems from the contribution of the jumps, is nonlocal: it is taken over the whole, two-dimensional asset price domain. In general, (semi-)closed analytical solutions to this PIDE

*Department of Mathematics, University of Antwerp, Middelheimlaan 1, B-2020 Antwerp, Belgium. Email: {karel.inhout,pieter.lamotte}@uantwerpen.be.

are not available in the literature. Accordingly, in the present paper, we investigate the effective numerical solution of the two-dimensional time-dependent Kou PIDE.

For the numerical solution, we follow the well-known and general method of lines (MOL) approach. The two-dimensional Kou PIDE is first discretized in space by finite differences, and the resulting large, semidiscrete system of ordinary differential equations (ODEs) is subsequently discretized in time by a suitable implicit time stepping scheme. The main challenges for the efficient and stable numerical solution are the treatment of the two-dimensional integral part and the treatment of the two-dimensional PDE part, which includes a mixed spatial derivative term.

Spatial discretization of the PIDE leads to a large, dense matrix for the integral part. In each time step of the schemes under consideration, products of this matrix with one or more given vectors need to be computed, which can form a computational burden. For the one-dimensional Kou PIDE, however, Toivanen [36] derived a simple algorithm for evaluating these matrix-vector products that has optimal computational cost. A key result of our paper is a generalization of Toivanen's algorithm to the two-dimensional Kou PIDE that maintains optimal computational cost.

For the temporal discretization of semidiscretized one-dimensional PIDEs arising in financial option valuation under jump-diffusion processes with finite activity jumps, various authors have proposed operator splitting schemes where the (stiff) PDE part is handled implicitly and the (nonstiff) integral part explicitly. Cont & Voltchkova [8] considered an *implicit-explicit (IMEX)* splitting scheme where the PDE part is handled by the backward Euler method and the integral part by the forward Euler method. This IMEX Euler scheme is only first-order consistent. A variety of higher-order IMEX schemes for PIDEs in finance has been studied since, e.g. by Briani, Natalini & Russo [5], Feng & Linetsky [10], Kwon & Lee [28] and Salmi & Toivanen [32]. The latter authors proposed the IMEX CNAB scheme, where the PDE part is treated by the Crank–Nicolson method and the integral part by the second-order Adams–Bashforth method. The IMEX CNAB scheme has been successfully applied to two-dimensional option valuation PIDEs in e.g. [21, 33].

Tavella & Randall [35] and d'Halluin, Forsyth & Vetzal [9] considered an alternative approach where the PDE part is treated by the Crank–Nicolson method and a fixed-point iteration on the integral part is performed in each time step. This approach has been applied to two-dimensional option valuation PIDEs in Clift & Forsyth [6], including the two-dimensional Kou PIDE. When the number of fixed-point iterations is frozen, one arrives at a particular IMEX scheme.

For the efficient temporal discretization of semidiscrete two-dimensional PIDEs, a subsequent important improvement is obtained by using, instead of the Crank–Nicolson method, an *alternating direction implicit (ADI)* splitting scheme for the two-dimensional PDE part. In the computational finance literature, a range of effective, second-order ADI schemes has been developed and analyzed for multi-dimensional PDEs (without integral part), where in each time step the implicit unidirectional stages are combined with explicit stages involving the mixed derivative terms, see e.g. [19, 21]. In this paper, we consider the well-established modified Craig–Sneyd (MCS) scheme, introduced by in 't Hout & Welfert [24], and the stabilizing correction two-step Adams-type scheme called SC2A, constructed by Hundsdorfer & in 't Hout [14].

The direct adaptation of ADI schemes for PDEs to PIDEs in finance has first been studied by Kaushansky, Lipton & Reisinger [26] and next by in 't Hout & Toivanen [22]. Here the implicit unidirectional stages are blended with explicit stages involving both the mixed derivative terms and the integral part, leading again to second-order schemes. We note that an efficient, parallel implementation of the schemes developed in [22] has been designed by Ghosh & Mishra [13] who apply a parallel cyclic reduction algorithm.

Boen & in 't Hout [4] recently investigated a collection of seven contemporary operator splitting schemes of both the IMEX and the ADI kind in the application to the two-dimensional Merton PIDE for the values of two-asset options. Here the numerical evaluation of the integral term has been done by means of a FFT-type algorithm, following e.g. [1, 2, 6, 9, 33]. Based on analytical and numerical evidence in [4, 22] in the case of the two-dimensional Merton and Bates PIDEs, it is concluded that, among the schemes under consideration, the adaptation of the MCS scheme introduced in [22] that deals with the integral part in a two-step Adams–Bashforth fashion is preferable.

In the present paper we consider for the two-dimensional Kou PIDE the same collection of operator splitting schemes as in [4]. For the numerical evaluation of the double integral part, a generalization of the algorithm of Toivanen [36] is derived that has optimal computational cost. This algorithm is simple to implement, requires little memory usage and is computationally much faster than the FFT-type algorithm mentioned above, cf. [36]. As a representative example, we consider the approximation of European put-on-the-average option values, together with their Greeks. An outline of the rest of this paper is as follows.

In Section 2 the two-dimensional Kou PIDE is formulated. Section 3 deals with its spatial discretization. First, in Subsection 3.1, the two-dimensional PDE part is considered and a second-order finite difference discretization on a suitable nonuniform spatial grid is described. Next, in Subsection 3.2, we present the first main contribution of this paper. A common, second-order spatial discretization of the double integral part is employed and for its highly efficient evaluation we derive an extension of the algorithm proposed by Toivanen [36]. It is shown that the computational cost of the extension is directly proportional to the number of spatial grid points, which is optimal. Section 4 subsequently concerns the temporal discretization of the obtained semidiscrete two-dimensional Kou PIDE. Here the seven contemporary operator splitting schemes of the IMEX and ADI kind from [4] are considered. Each of these schemes conveniently treats the integral part in an explicit manner, where its fast evaluation is performed by the algorithm derived in Subsection 3.2. A stability analysis of the operator splitting schemes pertinent to two-dimensional PIDEs is given in Section 5. In Section 6 ample numerical experiments are presented. Here European put-on-the-average option values, together with their Greeks Delta and Gamma, are considered and we examine in detail the temporal discretization errors and performance of the different operator splitting schemes. The final Section 7 gives conclusions.

2 The two-dimensional Kou PIDE

Under the two-asset Kou jump-diffusion model, the value $v = v(s_1, s_2, t)$ of a European-style option with maturity date $T > 0$ and s_i ($i = 1, 2$) representing the price of asset i at time $\tau = T - t$, satisfies the following PIDE:

$$\begin{aligned} \frac{\partial v}{\partial t} = & \frac{1}{2}\sigma_1^2 s_1^2 \frac{\partial^2 v}{\partial s_1^2} + \rho\sigma_1\sigma_2 s_1 s_2 \frac{\partial^2 v}{\partial s_1 \partial s_2} + \frac{1}{2}\sigma_2^2 s_2^2 \frac{\partial^2 v}{\partial s_2^2} + (r - \lambda\kappa_1)s_1 \frac{\partial v}{\partial s_1} + (r - \lambda\kappa_2)s_2 \frac{\partial v}{\partial s_2} \\ & - (r + \lambda)v + \lambda \int_0^\infty \int_0^\infty f(y_1, y_2)v(s_1 y_1, s_2 y_2, t) dy_1 dy_2 \end{aligned} \quad (2.1)$$

whenever $s_1 > 0$, $s_2 > 0$, $0 < t \leq T$. Here r is the risk-free interest rate, $\sigma_i > 0$ ($i = 1, 2$) is the instantaneous volatility for asset i conditional on the event that no jumps occur, and ρ is the correlation coefficient of the two underlying standard Brownian motions. Next, λ is the jump intensity of the underlying Poisson arrival process, and κ_i ($i = 1, 2$) is the expected relative jump size for asset i . The function f is the joint probability density function of two independent random variables possessing log-double-exponential distributions [27],

$$f(y_1, y_2) = \begin{cases} q_1 q_2 \eta_{q_1} \eta_{q_2} y_1^{\eta_{q_1}-1} y_2^{\eta_{q_2}-1} & (0 < y_1, y_2 < 1), \\ p_1 q_2 \eta_{p_1} \eta_{q_2} y_1^{-\eta_{p_1}-1} y_2^{\eta_{q_2}-1} & (y_1 \geq 1, 0 < y_2 < 1), \\ q_1 p_2 \eta_{q_1} \eta_{p_2} y_1^{\eta_{q_1}-1} y_2^{-\eta_{p_2}-1} & (0 < y_1 < 1, y_2 \geq 1), \\ p_1 p_2 \eta_{p_1} \eta_{p_2} y_1^{-\eta_{p_1}-1} y_2^{-\eta_{p_2}-1} & (y_1, y_2 \geq 1). \end{cases} \quad (2.2)$$

The parameters $p_i, q_i, \eta_{p_i}, \eta_{q_i}$ are all positive constants with $p_i + q_i = 1$ and $\eta_{p_i} > 1$. It holds that

$$\kappa_i = \frac{p_i \eta_{p_i}}{\eta_{p_i} - 1} + \frac{q_i \eta_{q_i}}{\eta_{q_i} + 1} - 1 \quad (i = 1, 2).$$

For (2.1), the initial condition is given by

$$v(s_1, s_2, 0) = \phi(s_1, s_2),$$

where ϕ denotes the payoff function of the option. As a typical example, we consider in this paper a European put-on-the-average option, which has the payoff function

$$\phi(s_1, s_2) = \max\left(0, K - \frac{s_1 + s_2}{2}\right) \quad (2.3)$$

with strike price $K > 0$. Its graph is shown in Figure 1. Concerning the boundary condition, it holds that the PIDE (2.1) is itself satisfied on the two sides $s_1 = 0$ and $s_2 = 0$, respectively.

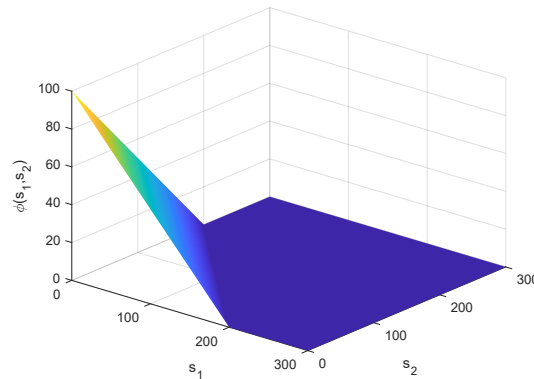


Figure 1: Payoff put-on-the-average option with $K = 100$.

3 Spatial discretization

For the numerical solution of the initial-boundary value problem for (2.1) we employ the popular method of lines (MOL) approach. This approach consists of two consecutive steps [15]: first the PIDE (2.1) is discretized in space and subsequently in time. This Section 3 deals with the spatial discretization. In the next Section 4 we shall consider the temporal discretization.

3.1 Convection-diffusion-reaction part

For the numerical solution, the spatial domain is truncated to a bounded set $[0, S_{\max}] \times [0, S_{\max}]$ with fixed value S_{\max} chosen sufficiently large. On the two far sides $s_1 = S_{\max}$ and $s_2 = S_{\max}$ a linear boundary condition is taken, which is well-known in finance,

$$\frac{\partial^2 v}{\partial s_1^2} = 0 \quad (\text{if } s_1 = S_{\max}) \quad \text{and} \quad \frac{\partial^2 v}{\partial s_2^2} = 0 \quad (\text{if } s_2 = S_{\max}). \quad (3.1)$$

In this subsection we describe the finite difference discretization of the convection-diffusion-reaction part of the PIDE (2.1), specified by

$$\mathcal{D}v = \frac{1}{2}\sigma_1^2 s_1^2 \frac{\partial^2 v}{\partial s_1^2} + \rho\sigma_1\sigma_2 s_1 s_2 \frac{\partial^2 v}{\partial s_1 \partial s_2} + \frac{1}{2}\sigma_2^2 s_2^2 \frac{\partial^2 v}{\partial s_2^2} + (r - \lambda\kappa_1)s_1 \frac{\partial v}{\partial s_1} + (r - \lambda\kappa_2)s_2 \frac{\partial v}{\partial s_2} - (r + \lambda)v.$$

The semidiscretization of this part is common and similar to that in e.g. [4].

Let integers $m_1, m_2 \geq 1$ be given. The option value function v is approximated at a nonuniform, Cartesian set of spatial grid points,

$$(s_{1,i}, s_{2,j}) \in [0, S_{\max}] \times [0, S_{\max}] \quad (0 \leq i \leq m_1, 0 \leq j \leq m_2),$$

with $s_{1,0} = s_{2,0} = 0$ and $s_{1,m_1} = s_{2,m_2} = S_{\max}$. The nonuniform grid in each spatial direction is defined through a smooth transformation of an artificial uniform grid, such that relatively many

grid points are placed in a region of financial and numerical interest. Figure 2 shows a sample spatial grid if $m_1 = m_2 = 50$, $K = 100$ and $S_{\max} = 5K$.

Let integer $m \geq 1$ and parameter $d > 0$. Consider equidistant points $0 = \xi_0 < \xi_1 < \dots < \xi_m = \xi_{\max}$ where

$$\xi_{\max} = \xi_{\text{int}} + \sinh^{-1} \left(\frac{S_{\max}}{d} - \xi_{\text{int}} \right) \quad \text{and} \quad \xi_{\text{int}} = \frac{2K}{d}.$$

Then in each spatial direction a nonuniform mesh $0 = s_0 < s_1 < \dots < s_m = S_{\max}$ is constructed by the smooth transformation $s_i = \varphi(\xi_i)$ ($0 \leq i \leq m$) with

$$\varphi(\xi) = \begin{cases} d\xi & (0 \leq \xi \leq \xi_{\text{int}}), \\ 2K + d \sinh(\xi - \xi_{\text{int}}) & (\xi_{\text{int}} < \xi \leq \xi_{\max}). \end{cases}$$

This mesh for s is uniform inside the interval $[0, 2K]$ and nonuniform outside. The parameter d controls the fraction of points s_i that lie inside. In this paper we (heuristically) choose $d = K/10$, such that the largest fraction is inside $[0, 2K]$.

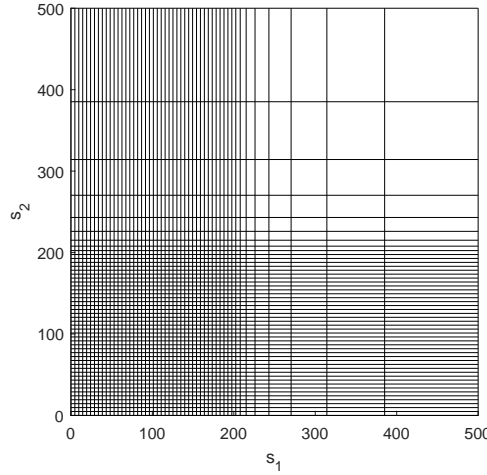


Figure 2: Sample spatial grid for $m_1 = m_2 = 50$, $K = 100$, $S_{\max} = 5K$.

Define mesh widths $h_i = s_i - s_{i-1}$ ($1 \leq i \leq m$) and let $u : [0, S_{\max}] \rightarrow \mathbb{R}$ be any given smooth function. For approximating the first and second derivatives of u , the following second-order central finite difference formulas are used:

$$u'(s_i) \approx \omega_{i,-1}u(s_{i-1}) + \omega_{i,0}u(s_i) + \omega_{i,1}u(s_{i+1}),$$

with

$$\omega_{i,-1} = \frac{-h_{i+1}}{h_i(h_i + h_{i+1})}, \quad \omega_{i,0} = \frac{h_{i+1} - h_i}{h_i h_{i+1}}, \quad \omega_{i,1} = \frac{h_i}{h_{i+1}(h_i + h_{i+1})}$$

and

$$u''(s_i) \approx \omega_{i,-1}u(s_{i-1}) + \omega_{i,0}u(s_i) + \omega_{i,1}u(s_{i+1}),$$

with

$$\omega_{i,-1} = \frac{2}{h_i(h_i + h_{i+1})}, \quad \omega_{i,0} = \frac{-2}{h_i h_{i+1}}, \quad \omega_{i,1} = \frac{2}{h_{i+1}(h_i + h_{i+1})}$$

whenever $1 \leq i \leq m-1$. For $i = 0$ no finite difference formulas are needed, due to the degeneracy of $\mathcal{D}v$ at the zero boundaries. For $i = m$, the first derivative is discretized by the first-order backward finite difference formula and the second derivative is equal to zero by the linear boundary condition

(3.1). Concerning the mixed derivative term in $\mathcal{D}v$, this is approximated by successively applying the relevant finite difference formulas for the first derivative in the two spatial directions.

Let $V_{i,j}(t)$ denote the semidiscrete approximation to $v(s_{1,i}, s_{2,j}, t)$ for $0 \leq i \leq m_1$, $0 \leq j \leq m_2$ and define the vector

$$V(t) = (V_{0,0}(t), V_{1,0}(t), \dots, V_{m_1-1, m_2}(t), V_{m_1, m_2}(t))^\top \in \mathbb{R}^{(m_1+1)(m_2+1)}.$$

The semidiscretized convection-diffusion-reaction part $\mathcal{D}v$ of PIDE (2.1) is then given by

$$A^{(D)}V(t)$$

with matrix

$$A^{(D)} = A^{(M)} + A_1 + A_2,$$

where

$$\begin{aligned} A^{(M)} &= \rho\sigma_1\sigma_2 \left(X_2 D_2^{(1)} \right) \otimes \left(X_1 D_1^{(1)} \right), \\ A_1 &= I_2 \otimes \left(\frac{1}{2}\sigma_1^2 X_1^2 D_1^{(2)} + (r - \lambda\kappa_1) X_1 D_1^{(1)} - \frac{1}{2}(r + \lambda) I_1 \right), \\ A_2 &= \left(\frac{1}{2}\sigma_2^2 X_2^2 D_2^{(2)} + (r - \lambda\kappa_2) X_2 D_2^{(1)} - \frac{1}{2}(r + \lambda) I_2 \right) \otimes I_1. \end{aligned}$$

Here I_k , X_k , $D_k^{(l)}$ are given $(m_k + 1) \times (m_k + 1)$ matrices for $k, l \in \{1, 2\}$ with I_k being the identity matrix, X_k being the diagonal matrix

$$X_k = \text{diag}(s_{k,0}, s_{k,1}, \dots, s_{k,m_k})$$

and $D_k^{(l)}$ the matrix representing numerical differentiation of order l in the k -th spatial direction by the relevant finite difference formula above. The matrix $A^{(M)}$ corresponds to the mixed derivative term in $\mathcal{D}v$ and A_k corresponds to all derivative terms in the k -th spatial direction ($k = 1, 2$), where the reaction term has been distributed evenly across A_1 and A_2 . These matrices are all sparse. In particular, A_1 and A_2 are (essentially) tridiagonal.

3.2 Integral part

In the following we consider discretization of the double integral

$$\mathcal{J} = \lambda \int_0^\infty \int_0^\infty f(y_1, y_2) v(s_1 y_1, s_2 y_2, t) dy_1 dy_2 \quad (3.2)$$

on the spatial grid from Subsection 3.1. For its efficient evaluation, we derive an extension of the algorithm proposed by Toivanen [36] for the special case of the one-dimensional Kou model.

Assume $s_1, s_2 > 0$ are given. A change of variables $y_i = z_i/s_i$ ($i = 1, 2$) yields

$$\mathcal{J} = \lambda \int_0^\infty \int_0^\infty f\left(\frac{z_1}{s_1}, \frac{z_2}{s_2}\right) v(z_1, z_2, t) \frac{dz_1 dz_2}{s_1 s_2}.$$

The density function f is defined on a partition of four sets of the first quadrant in the real plane, see (2.2). It follows that \mathcal{J} is decomposed into four integrals as $\mathcal{J} = \mathcal{J}_1 + \mathcal{J}_2 + \mathcal{J}_3 + \mathcal{J}_4$, where

$$\begin{aligned} \mathcal{J}_1 &= \lambda q_1 q_2 \eta_{q_1} \eta_{q_2} s_1^{-\eta_{q_1}} s_2^{-\eta_{q_2}} \int_0^{s_2} \int_0^{s_1} z_1^{\eta_{q_1}-1} z_2^{\eta_{q_2}-1} v(z_1, z_2, t) dz_1 dz_2, \\ \mathcal{J}_2 &= \lambda p_1 q_2 \eta_{p_1} \eta_{q_2} s_1^{\eta_{p_1}} s_2^{-\eta_{q_2}} \int_0^{s_2} \int_{s_1}^\infty z_1^{-\eta_{p_1}-1} z_2^{\eta_{q_2}-1} v(z_1, z_2, t) dz_1 dz_2, \\ \mathcal{J}_3 &= \lambda q_1 p_2 \eta_{q_1} \eta_{p_2} s_1^{-\eta_{q_1}} s_2^{\eta_{p_2}} \int_{s_2}^\infty \int_0^{s_1} z_1^{\eta_{q_1}-1} z_2^{-\eta_{p_2}-1} v(z_1, z_2, t) dz_1 dz_2, \\ \mathcal{J}_4 &= \lambda p_1 p_2 \eta_{p_1} \eta_{p_2} s_1^{\eta_{p_1}} s_2^{\eta_{p_2}} \int_{s_2}^\infty \int_{s_1}^\infty z_1^{-\eta_{p_1}-1} z_2^{-\eta_{p_2}-1} v(z_1, z_2, t) dz_1 dz_2. \end{aligned}$$

We first consider discretization of the integral \mathcal{J}_1 . Upon writing

$$\psi_1(s_1, s_2) = \lambda q_1 q_2 \eta_{q_1} \eta_{q_2} s_1^{-\eta_{q_1}} s_2^{-\eta_{q_2}} \quad \text{and} \quad \varphi_1(z_1, z_2) = z_1^{\eta_{q_1}-1} z_2^{\eta_{q_2}-1},$$

we have

$$\mathcal{J}_1 = \psi_1(s_1, s_2) \int_0^{s_2} \int_0^{s_1} \varphi_1(z_1, z_2) v(z_1, z_2, t) dz_1 dz_2. \quad (3.3)$$

For $1 \leq i \leq m_1$, $1 \leq j \leq m_2$ let

$$\mathcal{J}_{1,ij} = \psi_1(s_{1,i}, s_{2,j}) \int_0^{s_{2,j}} \int_0^{s_{1,i}} \varphi_1(z_1, z_2) v(z_1, z_2, t) dz_1 dz_2$$

denote the value of \mathcal{J}_1 at the spatial grid point $(s_{1,i}, s_{2,j})$. Define

$$\mathcal{G}_{1,kl} = \int_{s_{2,l-1}}^{s_{2,l}} \int_{s_{1,k-1}}^{s_{1,k}} \varphi_1(z_1, z_2) v(z_1, z_2, t) dz_1 dz_2$$

whenever $1 \leq k \leq m_1$, $1 \leq l \leq m_2$. Then the following useful expression for $\mathcal{J}_{1,ij}$ in terms of a double cumulative sum is obtained,

$$\mathcal{J}_{1,ij} = \psi_1(s_{1,i}, s_{2,j}) \sum_{k=1}^i \sum_{l=1}^j \mathcal{G}_{1,kl} \quad (1 \leq i \leq m_1, 1 \leq j \leq m_2). \quad (3.4)$$

Notice the obvious but important fact that the $\mathcal{G}_{1,kl}$ are independent of the indices i and j . Hence, if all values $\mathcal{G}_{1,kl}$ are given, then computing the double cumulative sums in (3.4) for all i, j can be done in, to leading order, just $2m_1m_2$ additions.

We subsequently construct approximations $G_{1,kl}$ to $\mathcal{G}_{1,kl}$ ($1 \leq k \leq m_1$, $1 \leq l \leq m_2$) and define the approximation to $\mathcal{J}_{1,ij}$ by

$$J_{1,ij} = \psi_1(s_{1,i}, s_{2,j}) \sum_{k=1}^i \sum_{l=1}^j G_{1,kl} \quad (1 \leq i \leq m_1, 1 \leq j \leq m_2). \quad (3.5)$$

For any given k, l with $1 \leq k \leq m_1$, $1 \leq l \leq m_2$ consider the natural choice of bilinear interpolation to approximate $v(z_1, z_2, t)$ on the (z_1, z_2) -domain $[s_{1,k-1}, s_{1,k}] \times [s_{2,l-1}, s_{2,l}]$:

$$\tilde{v}_{kl}(z_1, z_2, t) = \ell_{kl}^{00}(z_1, z_2) V_{k-1, l-1}(t) + \ell_{kl}^{10}(z_1, z_2) V_{k, l-1}(t) + \ell_{kl}^{01}(z_1, z_2) V_{k-1, l}(t) + \ell_{kl}^{11}(z_1, z_2) V_{k, l}(t)$$

with weights

$$\begin{aligned} \ell_{kl}^{00}(z_1, z_2) &= (s_{1,k} - z_1)(s_{2,l} - z_2)/\delta_{kl}, \\ \ell_{kl}^{10}(z_1, z_2) &= (z_1 - s_{1,k-1})(s_{2,l} - z_2)/\delta_{kl}, \\ \ell_{kl}^{01}(z_1, z_2) &= (s_{1,k} - z_1)(z_2 - s_{2,l-1})/\delta_{kl}, \\ \ell_{kl}^{11}(z_1, z_2) &= (z_1 - s_{1,k-1})(z_2 - s_{2,l-1})/\delta_{kl}, \end{aligned}$$

where $\delta_{kl} = \Delta s_{1,k} \Delta s_{2,l}$ and $\Delta s_{1,k} = s_{1,k} - s_{1,k-1}$, $\Delta s_{2,l} = s_{2,l} - s_{2,l-1}$. Then we define

$$G_{1,kl} = \int_{s_{2,l-1}}^{s_{2,l}} \int_{s_{1,k-1}}^{s_{1,k}} \varphi_1(z_1, z_2) \tilde{v}_{kl}(z_1, z_2, t) dz_1 dz_2.$$

A straightforward calculation yields the simple, convenient formula

$$G_{1,kl} = \gamma_{1,kl}^{00} V_{k-1, l-1}(t) + \gamma_{1,kl}^{10} V_{k, l-1}(t) + \gamma_{1,kl}^{01} V_{k-1, l}(t) + \gamma_{1,kl}^{11} V_{k, l}(t) \quad (3.6)$$

with

$$\begin{aligned} \gamma_{1,kl}^{00} &= (s_{1,k} s_{2,l} \zeta_{1,kl}^{00} - s_{2,l} \zeta_{1,kl}^{10} - s_{1,k} \zeta_{1,kl}^{01} + \zeta_{1,kl}^{11})/\delta_{kl}, \\ \gamma_{1,kl}^{10} &= (-s_{1,k-1} s_{2,l} \zeta_{1,kl}^{00} + s_{2,l} \zeta_{1,kl}^{10} + s_{1,k-1} \zeta_{1,kl}^{01} - \zeta_{1,kl}^{11})/\delta_{kl}, \\ \gamma_{1,kl}^{01} &= (-s_{1,k} s_{2,l-1} \zeta_{1,kl}^{00} + s_{2,l-1} \zeta_{1,kl}^{10} + s_{1,k} \zeta_{1,kl}^{01} - \zeta_{1,kl}^{11})/\delta_{kl}, \\ \gamma_{1,kl}^{11} &= (s_{1,k-1} s_{2,l-1} \zeta_{1,kl}^{00} - s_{2,l-1} \zeta_{1,kl}^{10} - s_{1,k-1} \zeta_{1,kl}^{01} + \zeta_{1,kl}^{11})/\delta_{kl} \end{aligned}$$

and

$$\zeta_{1,kl}^{ab} = \int_{s_{2,l-1}}^{s_{2,l}} \int_{s_{1,k-1}}^{s_{1,k}} \varphi_1(z_1, z_2) z_1^a z_2^b dz_1 dz_2 = \frac{\left(s_{1,k}^{a+\eta_{q_1}} - s_{1,k-1}^{a+\eta_{q_1}} \right) \left(s_{2,l}^{b+\eta_{q_2}} - s_{2,l-1}^{b+\eta_{q_2}} \right)}{(a + \eta_{q_1})(b + \eta_{q_2})}$$

for $a, b \in \{0, 1\}$.

The coefficients $\gamma_{1,kl}^{ab}$ are completely determined by the Kou parameters and the spatial grid. Since they are independent of t , they can be computed upfront, before the time discretization. Clearly, for any given vector $V(t)$, the computation of $G_{1,kl}$ by (3.6) for all k, l requires $3m_1m_2$ additions and $4m_1m_2$ multiplications. Noticing that the values of ψ_1 in (3.5) can also be computed upfront, it follows that the number of basic arithmetic operations to compute all approximations $J_{1,ij}$ ($1 \leq i \leq m_1, 1 \leq j \leq m_2$) by (3.5) is, to leading order, equal to $10m_1m_2$.

The discretization and efficient evaluation of the other three integrals is done completely analogously. In the relevant derivation, v is approximated by zero outside the spatial domain $[0, S_{\max}] \times [0, S_{\max}]$. Write

$$\begin{aligned} \psi_2(s_1, s_2) &= \lambda p_1 q_2 \eta_{p_1} \eta_{q_2} s_1^{\eta_{p_1}} s_2^{-\eta_{q_2}}, \\ \psi_3(s_1, s_2) &= \lambda q_1 p_2 \eta_{q_1} \eta_{p_2} s_1^{-\eta_{q_1}} s_2^{\eta_{p_2}}, \\ \psi_4(s_1, s_2) &= \lambda p_1 p_2 \eta_{p_1} \eta_{p_2} s_1^{\eta_{p_1}} s_2^{\eta_{p_2}}. \end{aligned}$$

Let $1 \leq i \leq m_1, 1 \leq j \leq m_2$. Then the approximations of $\mathcal{J}_2, \mathcal{J}_3, \mathcal{J}_4$ at the spatial grid point $(s_{1,i}, s_{2,j})$ are given by, respectively, the double cumulative sums

$$\begin{aligned} J_{2,ij} &= \psi_2(s_{1,i}, s_{2,j}) \sum_{k=i+1}^{m_1} \sum_{l=1}^j G_{2,kl}, \\ J_{3,ij} &= \psi_3(s_{1,i}, s_{2,j}) \sum_{k=1}^i \sum_{l=j+1}^{m_2} G_{3,kl}, \\ J_{4,ij} &= \psi_4(s_{1,i}, s_{2,j}) \sum_{k=i+1}^{m_1} \sum_{l=j+1}^{m_2} G_{4,kl} \end{aligned}$$

with the usual convention that empty sums are equal to zero. For $2 \leq \nu \leq 4, 1 \leq k \leq m_1, 1 \leq l \leq m_2$ we obtain

$$G_{\nu,kl} = \gamma_{\nu,kl}^{00} V_{k-1,l-1}(t) + \gamma_{\nu,kl}^{10} V_{k,l-1}(t) + \gamma_{\nu,kl}^{01} V_{k-1,l}(t) + \gamma_{\nu,kl}^{11} V_{k,l}(t)$$

with

$$\begin{aligned} \gamma_{\nu,kl}^{00} &= (s_{1,k} s_{2,l} \zeta_{\nu,kl}^{00} - s_{2,l} \zeta_{\nu,kl}^{10} - s_{1,k} \zeta_{\nu,kl}^{01} + \zeta_{\nu,kl}^{11}) / \delta_{kl}, \\ \gamma_{\nu,kl}^{10} &= (-s_{1,k-1} s_{2,l} \zeta_{\nu,kl}^{00} + s_{2,l} \zeta_{\nu,kl}^{10} + s_{1,k-1} \zeta_{\nu,kl}^{01} - \zeta_{\nu,kl}^{11}) / \delta_{kl}, \\ \gamma_{\nu,kl}^{01} &= (-s_{1,k} s_{2,l-1} \zeta_{\nu,kl}^{00} + s_{2,l-1} \zeta_{\nu,kl}^{10} + s_{1,k} \zeta_{\nu,kl}^{01} - \zeta_{\nu,kl}^{11}) / \delta_{kl}, \\ \gamma_{\nu,kl}^{11} &= (s_{1,k-1} s_{2,l-1} \zeta_{\nu,kl}^{00} - s_{2,l-1} \zeta_{\nu,kl}^{10} - s_{1,k-1} \zeta_{\nu,kl}^{01} + \zeta_{\nu,kl}^{11}) / \delta_{kl} \end{aligned}$$

where

$$\begin{aligned} \zeta_{2,kl}^{ab} &= \frac{\left(s_{1,k}^{a-\eta_{p_1}} - s_{1,k-1}^{a-\eta_{p_1}} \right) \left(s_{2,l}^{b+\eta_{q_2}} - s_{2,l-1}^{b+\eta_{q_2}} \right)}{(a - \eta_{p_1})(b + \eta_{q_2})}, \\ \zeta_{3,kl}^{ab} &= \frac{\left(s_{1,k}^{a+\eta_{q_1}} - s_{1,k-1}^{a+\eta_{q_1}} \right) \left(s_{2,l}^{b-\eta_{p_2}} - s_{2,l-1}^{b-\eta_{p_2}} \right)}{(a + \eta_{q_1})(b - \eta_{p_2})}, \\ \zeta_{4,kl}^{ab} &= \frac{\left(s_{1,k}^{a-\eta_{p_1}} - s_{1,k-1}^{a-\eta_{p_1}} \right) \left(s_{2,l}^{b-\eta_{p_2}} - s_{2,l-1}^{b-\eta_{p_2}} \right)}{(a - \eta_{p_1})(b - \eta_{p_2})} \end{aligned}$$

for $a, b \in \{0, 1\}$.

On the boundary part $\{(s_1, 0) : s_1 > 0\}$ the double integral (3.2) reduces to the single integral

$$\mathcal{J} = \lambda \int_0^\infty f_1(y_1)v(s_1 y_1, 0, t)dy_1. \quad (3.7)$$

The discretization and efficient evaluation of this integral, which arises in the one-dimensional Kou PIDE, has been constructed by Toivanen [36]. For completeness, we include the result here. Assume $s_1 > 0$. Then for (3.7) there holds $\mathcal{J} = \mathcal{J}_1 + \mathcal{J}_2$, where

$$\mathcal{J}_1 = \lambda \int_0^{s_1} f_1\left(\frac{z_1}{s_1}\right)v(z_1, 0, t)\frac{dz_1}{s_1} \quad \text{and} \quad \mathcal{J}_2 = \lambda \int_{s_1}^\infty f_1\left(\frac{z_1}{s_1}\right)v(z_1, 0, t)\frac{dz_1}{s_1}.$$

Write

$$\psi_1(s_1) = \lambda q_1 \eta_{q_1} s_1^{-\eta_{q_1}} \quad \text{and} \quad \psi_2(s_1) = \lambda p_1 \eta_{p_1} s_1^{\eta_{p_1}}.$$

Let $1 \leq i \leq m_1$. Then the approximations of $\mathcal{J}_1, \mathcal{J}_2$ at the spatial grid point $(s_{1,i}, 0)$ are given by, respectively, the single cumulative sums

$$J_{1,i} = \psi_1(s_{1,i}) \sum_{k=1}^i G_{1,k} \quad \text{and} \quad J_{2,i} = \psi_2(s_{1,i}) \sum_{k=i+1}^{m_1} G_{2,k}.$$

For $1 \leq \nu \leq 2$, $1 \leq k \leq m_1$ we obtain, by employing linear interpolation,

$$G_{\nu,k} = \gamma_{\nu,k}^0 V_{k-1,0}(t) + \gamma_{\nu,k}^1 V_{k,0}(t)$$

with

$$\gamma_{\nu,k}^0 = (s_{1,k} \zeta_{\nu,k}^0 - \zeta_{\nu,k}^1) / \Delta s_{1,k} \quad \text{and} \quad \gamma_{\nu,k}^1 = (-s_{1,k-1} \zeta_{\nu,k}^0 + \zeta_{\nu,k}^1) / \Delta s_{1,k}$$

where

$$\zeta_{1,k}^a = \frac{s_{1,k}^{a+\eta_{q_1}} - s_{1,k-1}^{a+\eta_{q_1}}}{a + \eta_{q_1}} \quad \text{and} \quad \zeta_{2,k}^a = \frac{s_{1,k}^{a-\eta_{p_1}} - s_{1,k-1}^{a-\eta_{p_1}}}{a - \eta_{p_1}} \quad (a = 0, 1).$$

On the boundary part $\{(0, s_2) : s_2 > 0\}$ the double integral (3.2) reduces to the single integral

$$\mathcal{J} = \lambda \int_0^\infty f_2(y_2)v(0, s_2 y_2, t)dy_2 \quad (3.8)$$

and the discretization is performed completely similarly as above. Finally, at the spatial grid point $(s_1, s_2) = (0, 0)$ it holds that $\mathcal{J} \approx \lambda V_{0,0}(t)$.

From the above it follows that the number of basic arithmetic operations to compute, for any given t , the approximation to the double integral (3.2) on the full spatial grid is, to leading order, equal to $40m_1m_2$.

As an illustration, Table 1 shows the obtained CPU times (in seconds) for our implementation¹ of the acquired algorithm for approximating (3.2) for a single time t on the full spatial grid with $m_1 = m_2 = m$ and $m = 100, 200, \dots, 1000$ in the case of parameter set 1 from Section 6. It is readily verified from Table 1 that the CPU time behaves, for large m , directly proportional to m^2 , which agrees with the above theoretical result.

Table 1

CPU time vs. $m_1 = m_2 = m$ for the algorithm of Subsection 3.2 to approximate the integral (3.2).

m	100	200	300	400	500	600	700	800	900	1000
CPU time (s)	1.2e-3	2.9e-3	8.8e-3	2.3e-2	3.7e-2	5.2e-2	7.3e-2	9.7e-2	1.3e-1	1.6e-1

¹In Matlab version R2020b, on an Intel Core i7-8665U processor at 1.9 GHz with 16 GB memory.

3.3 Semidiscrete PIDE

Combining the above semidiscretizations for the convection-diffusion-reaction and integral parts of PIDE (2.1), the following large system of ODEs is obtained:

$$V'(t) = AV(t) \quad (0 < t \leq T), \quad (3.9)$$

where

$$A = A^{(D)} + A^{(J)} = A^{(M)} + A_1 + A_2 + A^{(J)}.$$

Even though we never actually compute it in this way, the approximation to the double integral (3.2) defined in Subsection 3.2 is formally denoted here by $A^{(J)}V(t)$ with given (full) matrix $A^{(J)}$.

The initial vector $V(0) = V^0$ is defined by pointwise evaluation of the payoff function ϕ on the spatial grid, except at those grid points that lie near to the line segment given by $s_1 + s_2 = 2K$ where ϕ is nonsmooth. It is well-known that using pointwise values of ϕ in such a region can lead to a deteriorated (spatial) convergence behavior, which can be alleviated by applying cell averaging. Accordingly, for $k = 1, 2$ let

$$\begin{aligned} s_{k,l+1/2} &= \frac{1}{2}(s_{k,l} + s_{k,l+1}) & \text{if } 0 \leq l < m, \\ h_{k,l+1/2} &= s_{k,l+1/2} - s_{k,l-1/2} & \text{if } 0 \leq l \leq m, \end{aligned}$$

with $s_{k,-1/2} = -s_{k,1/2}$ and $s_{k,m+1/2} = S_{\max}$. Then we define [19]

$$V_{i,j}(0) = \frac{1}{h_{1,i+1/2}h_{2,j+1/2}} \int_{s_{1,i-1/2}}^{s_{1,i+1/2}} \int_{s_{2,j-1/2}}^{s_{2,j+1/2}} \phi(s_1, s_2) ds_2 ds_1 \quad (3.10)$$

whenever the cell

$$[s_{1,i-1/2}, s_{1,i+1/2}) \times [s_{2,j-1/2}, s_{2,j+1/2})$$

has a nonempty intersection with the line segment $s_1 + s_2 = 2K$. Note that the double integral (3.10) is easily calculated.

4 Temporal discretization

For the temporal discretization of the semidiscrete PIDE (3.9) we study seven operator splitting schemes of the IMEX and ADI kind [4]. Let integer $N \geq 1$ be given and define step size $\Delta t = T/N$ and temporal grid points $t_n = n\Delta t$ for $n = 0, 1, 2, \dots, N$. Each of the following schemes generates an approximation V^n to $V(t_n)$ successively for $n = 1, 2, \dots, N$. Here the integral part of (3.9), corresponding to the matrix $A^{(J)}$, is always conveniently treated in an explicit manner and evaluated by applying the efficient algorithm derived in Subsection 3.2.

1. Crank–Nicolson Forward Euler (CNFE) scheme:

In this one-step IMEX method, the convection-diffusion-reaction part is handled implicitly by the Crank–Nicolson scheme and the integral part is treated in a simple, explicit Euler fashion:

$$\left(I - \frac{1}{2}\Delta t A^{(D)}\right) V^n = \left(I + \frac{1}{2}\Delta t A^{(D)}\right) V^{n-1} + \Delta t A^{(J)} V^{n-1}. \quad (4.1)$$

Due to the application of explicit Euler, the order² of the CNFE scheme is just equal to one.

²This means the classical order of consistency, i.e., for fixed nonstiff ODEs.

2. *Crank–Nicolson scheme with fixed-point iteration (CNFI):*

Tavella & Randall [35] and d’Halluin, Forsyth & Vetzal [9] proposed to combine the Crank–Nicolson scheme for the convection-diffusion-reaction part with a fixed-point iteration on the integral part:

$$\left(I - \frac{1}{2}\Delta t A^{(D)}\right) Y_k = \left(I + \frac{1}{2}\Delta t A^{(D)}\right) V^{n-1} + \frac{1}{2}\Delta t A^{(J)}(Y_{k-1} + V^{n-1}) \quad (4.2)$$

for $k = 1, 2, \dots, l$ and $V^n = Y_l$ with starting vector $Y_0 = V^{n-1}$. Numerical evidence in [6, 9] indicates that in general $l = 2$ or $l = 3$ iterations suffice. In the numerical experiments in Section 6 we shall consider a fixed number of $l = 2$ iterations. Then method (4.2) can be viewed as a one-step IMEX scheme, where the integral part is treated by the explicit trapezoidal rule, also called the modified Euler method. By Taylor expansion, it can be seen that its order is equal to two.

3. *Implicit-Explicit Trapezoidal Rule (IETR):*

Another blend of the implicit trapezoidal rule (Crank–Nicolson) for the convection-diffusion-reaction part and the explicit trapezoidal rule for the integral part has been considered in [19]:

$$\begin{cases} Y_0 = V^{n-1} + \Delta t (A^{(D)} + A^{(J)})V^{n-1}, \\ \widehat{Y}_0 = Y_0 + \frac{1}{2}\Delta t A^{(J)}(Y_0 - V^{n-1}), \\ Y_1 = \widehat{Y}_0 + \frac{1}{2}\Delta t A^{(D)}(Y_1 - V^{n-1}), \\ V^n = Y_1. \end{cases} \quad (4.3)$$

Method (4.3) also forms a one-step IMEX scheme with order equal to two. It is already well-known in the literature on the numerical solution of PDEs (without integral part), see e.g. Hundsdorfer & Verwer [15]. Notice that the first two internal stages Y_0, \widehat{Y}_0 are explicit, whereas the third internal stage Y_1 is implicit.

4. *Crank–Nicolson Adams–Bashforth (CNAB) scheme:*

The CNAB method has been amply considered in the literature on the numerical solution of PDEs as well, see e.g. [12, 15, 18]. It has been investigated for the numerical solution of PIDEs by Salmi & Toivanen [32] and Salmi, Toivanen & von Sydow [33]. The convection-diffusion-reaction part is again handled by the Crank–Nicolson scheme, but the integral part is now dealt with in a two-step Adams–Bashforth fashion:

$$\left(I - \frac{1}{2}\Delta t A^{(D)}\right) V^n = \left(I + \frac{1}{2}\Delta t A^{(D)}\right) V^{n-1} + \frac{1}{2}\Delta t A^{(J)}(3V^{n-1} - V^{n-2}). \quad (4.4)$$

Method (4.4) constitutes a two-step IMEX scheme and is of order equal to two. It is interesting to remark that (4.4) can also be viewed as obtained from (4.2), upon taking $l = 1$ and improved (linearly extrapolated) starting value $Y_0 = 2V^{n-1} - V^{n-2}$.

As for the spatial discretization, it is well-known that the nonsmoothness of the payoff function can have an unfavorable impact on the convergence behavior of the temporal discretization, even if cell averaging is applied, cf. [19]. For the Crank–Nicolson scheme a common approach to alleviate this has been proposed by Rannacher [31]. It consists of replacing (only) the first time step by two time steps with step size $\Delta t/2$ using the implicit Euler method, thus defining the approximation V^1 to $V(t_1)$. In the present case of two-dimensional PIDEs, the implicit Euler method can be computationally intensive. We therefore consider, for all four IMEX schemes above, the *IMEX Euler scheme* as the starting method:

$$\begin{aligned} \left(I - \frac{1}{2}\Delta t A^{(D)}\right) V^{\frac{1}{2}} &= V^0 + \frac{1}{2}\Delta t A^{(J)}V^0, \\ \left(I - \frac{1}{2}\Delta t A^{(D)}\right) V^1 &= V^{\frac{1}{2}} + \frac{1}{2}\Delta t A^{(J)}V^{\frac{1}{2}}. \end{aligned}$$

Clearly, in each of the IMEX schemes under consideration, linear systems need to be solved involving the matrix $I - \frac{1}{2}\Delta t A^{(D)}$. Whereas this matrix is sparse, with at most nine nonzero entries per row, it possesses a large bandwidth that is directly proportional to m_1 . With a view to obtaining a further reduction in computational work, we consider three recent operator splitting schemes for PIDEs that employ also the (directional) splitting $A^{(D)} = A^{(M)} + A_1 + A_2$ of the two-dimensional convection-diffusion-reaction part, such that only linear systems with tridiagonal matrices arise.

5. *One-step adaptation of the modified Craig-Sneyd (MCS) scheme:*

The MCS scheme is an ADI scheme that was introduced by in 't Hout & Welfert [24] for the numerical solution of PDEs containing mixed spatial derivative terms. The following, direct adaptation to PIDEs has recently been investigated by in 't Hout & Toivanen [22]:

$$\begin{cases} Y_0 = V^{n-1} + \Delta t (A^{(D)} + A^{(J)})V^{n-1}, \\ Y_j = Y_{j-1} + \theta \Delta t A_j (Y_j - V^{n-1}) \quad (j = 1, 2), \\ \hat{Y}_0 = Y_0 + \theta \Delta t (A^{(M)} + A^{(J)})(Y_2 - V^{n-1}), \\ \tilde{Y}_0 = \hat{Y}_0 + (\frac{1}{2} - \theta) \Delta t (A^{(D)} + A^{(J)})(Y_2 - V^{n-1}), \\ \tilde{Y}_j = \tilde{Y}_{j-1} + \theta \Delta t A_j (\tilde{Y}_j - V^{n-1}) \quad (j = 1, 2), \\ V^n = \tilde{Y}_2, \end{cases} \quad (4.5)$$

where $\theta > 0$ is a given parameter. Method (4.5) is of order two for any value θ . Here we make the common choice $\theta = \frac{1}{3}$, which is motivated by stability and accuracy results for two-dimensional problems, see e.g. [20, 22, 24, 25] and Section 5. It is easily verified that in (4.5) the integral part and mixed derivative term are both treated by the explicit trapezoidal rule. We note that the explicit stages \hat{Y}_0, \tilde{Y}_0 can be merged, so that the integral part is evaluated (just) twice per time step. The implicit stages Y_j, \tilde{Y}_j (for $j = 1, 2$) are often called stabilizing corrections. The four pertinent linear systems for these stages are tridiagonal and can be solved very efficiently by means of an a priori LU factorization. We mention that (4.5) is already applied in the first time step, i.e., for defining V^1 (thus IMEX Euler is not used here).

6. *Two-step adaptation of the MCS (MCS2) scheme:*

In [22] a second adaptation of the MCS scheme to PIDEs has been proposed where, instead of the explicit trapezoidal rule, the integral part is now handled in a two-step Adams-Bashforth fashion:

$$\begin{cases} X_0 = V^{n-1} + \Delta t A^{(D)} V^{n-1}, \\ Y_0 = X_0 + \frac{1}{2} \Delta t A^{(J)} (3V^{n-1} - V^{n-2}), \\ Y_j = Y_{j-1} + \theta \Delta t A_j (Y_j - V^{n-1}) \quad (j = 1, 2), \\ \hat{Y}_0 = Y_0 + \theta \Delta t A^{(M)} (Y_2 - V^{n-1}), \\ \tilde{Y}_0 = \hat{Y}_0 + (\frac{1}{2} - \theta) \Delta t A^{(D)} (Y_2 - V^{n-1}), \\ \tilde{Y}_j = \tilde{Y}_{j-1} + \theta \Delta t A_j (\tilde{Y}_j - V^{n-1}) \quad (j = 1, 2), \\ V^n = \tilde{Y}_2. \end{cases} \quad (4.6)$$

Method (4.6) is also of order two for any value θ . We choose again $\theta = \frac{1}{3}$ and, for starting this two-step method, define V^1 by (4.5).

7. *Stabilizing correction two-step Adams-type (SC2A) scheme:*

Hundsdofer & in 't Hout [14] recently studied a novel class of stabilizing correction multistep methods for the numerical solution of PDEs. We consider here a direct adaptation to PIDEs of a prominent member of this class, the two-step Adams-type scheme called SC2A:

$$\begin{cases} Y_0 = V^{n-1} + \Delta t (A^{(M)} + A^{(J)}) \sum_{i=1}^2 \hat{b}_i V^{n-i} + \Delta t (A_1 + A_2) \sum_{i=1}^2 \check{b}_i V^{n-i}, \\ Y_j = Y_{j-1} + \theta \Delta t A_j (Y_j - V^{n-1}) \quad (j = 1, 2), \\ V^n = Y_2, \end{cases} \quad (4.7)$$

with coefficients $(\hat{b}_1, \hat{b}_2) = (\frac{3}{2}, -\frac{1}{2})$ and $(\check{b}_1, \check{b}_2) = (\frac{3}{2} - \theta, -\frac{1}{2} + \theta)$. The integral part and mixed derivative term are now both handled by the two-step Adams–Bashforth scheme. Method (4.7) is again of order two for any value θ . Following [14], we take $\theta = \frac{3}{4}$, which is based upon stability and accuracy results. For starting (4.7), we define V^1 again by (4.5) with $\theta = \frac{1}{3}$

We conclude this section with a summary of the main characteristics of the seven operator splitting schemes in Table 2, indicating its order, whether it is a one- or a two-step scheme, the number of linear systems in each time step, and the number of evaluations of the integral part in each time step.

Table 2

Main characteristics of the seven operator splitting schemes (with $l \geq 2$).

	CNFE	CNFI	IETR	CNAB	MCS	MCS2	SC2A
order	1	2	2	2	2	2	2
one/two-step	1	1	1	2	1	2	2
linear systems	1	l	1	1	4	4	2
integral terms	1	l	2	1	2	1	1

5 Stability analysis

Let $\mu_0, \mu_1, \mu_2, \lambda_0$ denote any given complex numbers representing eigenvalues of the matrices $A^{(M)}, A_1, A_2, A^{(J)}$, respectively. For the stability analysis of the operator splitting schemes from Section 4 we consider the linear scalar test equation

$$V'(t) = (\mu_0 + \mu_1 + \mu_2 + \lambda_0) V(t). \quad (5.1)$$

Let $z_j = \mu_j \Delta t$ (for $j = 0, 1, 2$) and $w_0 = \lambda_0 \Delta t$ and write $w = z_0 + z_1 + z_2$, $p = (1 - \theta z_1)(1 - \theta z_2)$. Application of the three IMEX schemes (4.1), (4.2), (4.3) to test equation (5.1) yields a one-step linear recurrence relation of the form

$$V^n = R(w, w_0) V^{n-1},$$

where

$$\text{for (4.1): } R(w, w_0) = \frac{1 + \frac{1}{2}w + w_0}{1 - \frac{1}{2}w}, \quad (5.2)$$

$$\text{for (4.2): } R(w, w_0) = \left(\frac{\frac{1}{2}w_0}{1 - \frac{1}{2}w} \right)^l + \sum_{k=0}^{l-1} \left(\frac{\frac{1}{2}w_0}{1 - \frac{1}{2}w} \right)^k \cdot \frac{1 + \frac{1}{2}w + \frac{1}{2}w_0}{1 - \frac{1}{2}w}, \quad (5.3)$$

$$\text{for (4.3): } R(w, w_0) = \frac{1 + \frac{1}{2}w + w_0 + \frac{1}{2}(w + w_0)w_0}{1 - \frac{1}{2}w}. \quad (5.4)$$

Application of the IMEX scheme (4.4) to (5.1) yields a two-step linear recurrence relation

$$V^n = R_1(w, w_0) V^{n-1} + R_0(w, w_0) V^{n-2},$$

with

$$R_1(w, w_0) = \frac{1 + \frac{1}{2}w + \frac{3}{2}w_0}{1 - \frac{1}{2}w}, \quad (5.5)$$

$$R_0(w, w_0) = \frac{-\frac{1}{2}w_0}{1 - \frac{1}{2}w}. \quad (5.6)$$

Application of the ADI scheme (4.5) to (5.1) gives a one-step linear recurrence of the form

$$V^n = R(z_0, z_1, z_2, w_0) V^{n-1},$$

where

$$R(z_0, z_1, z_2, w_0) = 1 + \frac{w + w_0}{p} + \theta \frac{(z_0 + w_0)(w + w_0)}{p^2} + \left(\frac{1}{2} - \theta\right) \frac{(w + w_0)^2}{p^2}. \quad (5.7)$$

Application of the two ADI schemes (4.6), (4.7) to (5.1) gives a two-step linear recurrence

$$V^n = R_1(z_0, z_1, z_2, w_0) V^{n-1} + R_0(z_0, z_1, z_2, w_0) V^{n-2}.$$

Here, for (4.6),

$$R_1(z_0, z_1, z_2, w_0) = 1 + (w + \frac{3}{2}w_0) \left(\frac{1}{p} + \theta \frac{z_0}{p^2} + \left(\frac{1}{2} - \theta\right) \frac{w}{p^2} \right), \quad (5.8)$$

$$R_0(z_0, z_1, z_2, w_0) = -\frac{1}{2}w_0 \left(\frac{1}{p} + \theta \frac{z_0}{p^2} + \left(\frac{1}{2} - \theta\right) \frac{w}{p^2} \right). \quad (5.9)$$

Next, for (4.7),

$$R_1(z_0, z_1, z_2, w_0) = 1 + \frac{1}{p} \left(\hat{b}_1(z_0 + w_0) + \check{b}_1(z_1 + z_2) \right), \quad (5.10)$$

$$R_0(z_0, z_1, z_2, w_0) = \frac{1}{p} \left(\hat{b}_2(z_0 + w_0) + \check{b}_2(z_1 + z_2) \right). \quad (5.11)$$

In the stability analysis of ADI schemes for two-dimensional convection-diffusion equations with mixed derivative term (and without integral term), the following condition on z_0, z_1, z_2 plays a main role:

$$|z_0| \leq 2\sqrt{\Re z_1 \Re z_2}, \quad \Re z_1 \leq 0, \quad \Re z_2 \leq 0, \quad (5.12)$$

where \Re denotes the real part of a complex number. Condition (5.12) has been shown to hold [23] in the von Neumann framework where semidiscretization is performed by second-order central finite differences on uniform, Cartesian grids and periodic boundary condition. We note that it is readily seen that (5.12) implies $\Re w \leq 0$.

The subsequent stability results are relevant to the natural situation (for finite activity jumps) where $|\lambda_0|T$ is of moderate size. Our analysis relies upon a polynomial expansion in $w_0 = \lambda_0 \Delta t$. Such an argument has previously been employed in [22, 26] (cf. also e.g. [15, p.385,386] in a PDE context).

For stability of a one-step linear recurrence, we consider power-boundedness of R , and for stability of a two-step linear recurrence, power-boundedness of the 2×2 companion matrix

$$C = \begin{pmatrix} R_1 & R_0 \\ 1 & 0 \end{pmatrix}.$$

Denote by $\|\cdot\|$ the maximum norm for matrices. The first result deals with the IMEX schemes (4.1)–(4.4).

Theorem 5.1. *Let $l \geq 1$ and $c = \sum_{k=0}^{l-1} \left(\frac{1}{2}|\lambda_0|T\right)^k$. Then:*

- (a) *for the scheme (4.1) there holds $|R(w, w_0)^n| \leq e^{|\lambda_0|t_n}$,*
- (b) *for the scheme (4.2) there holds $|R(w, w_0)^n| \leq e^{c|\lambda_0|t_n}$,*
- (c) *for the scheme (4.3) there holds $|R(w, w_0)^n| \leq e^{|\lambda_0|t_n}$,*
- (d) *for the scheme (4.4) there holds $\|C(w, w_0)^n\| \leq e^{2|\lambda_0|t_n}$*

whenever $w \in \mathbb{C}$, $\Re w \leq 0$.

Proof. It is sufficient to prove the upper bounds for $n = 1$. Define $P = R(w, 0) = (1 + \frac{1}{2}w)(1 - \frac{1}{2}w)^{-1}$ and $Q = \frac{1}{2}(1 - \frac{1}{2}w)^{-1}$. Since $\Re w \leq 0$ we have $|P| \leq 1$ and $|Q| \leq \frac{1}{2}$.

(a) The scheme (4.1) is identical to (4.2) with $l = 1$ and the bound is given by part (b) with $l = 1$.

(b) Let $\omega = \frac{1}{2}|w_0| = \frac{1}{2}|\lambda_0| \Delta t$. For (4.2), one can write

$$R(w, w_0) = (w_0 Q)^l + \sum_{k=0}^{l-1} (w_0 Q)^k \cdot (P + w_0 Q).$$

It follows that

$$|R(w, w_0)| \leq \omega^l + \sum_{k=0}^{l-1} \omega^k (1 + \omega) = 1 + 2\omega \sum_{k=0}^{l-1} \omega^k \leq 1 + c|\lambda_0| \Delta t \leq e^{c|\lambda_0| \Delta t}.$$

(c) For (4.3), we have

$$R(w, w_0) = (1 + w_0)P + w_0^2 Q,$$

and hence

$$|R(w, w_0)| \leq 1 + |\lambda_0| \Delta t + \frac{1}{2}(|\lambda_0| \Delta t)^2 \leq e^{|\lambda_0| \Delta t}.$$

(d) For (4.4),

$$C(w, w_0) = \begin{pmatrix} P & 0 \\ 1 & 0 \end{pmatrix} + w_0 Q \begin{pmatrix} 3 & -1 \\ 0 & 0 \end{pmatrix}.$$

Consequently,

$$\|C(w, w_0)\| \leq 1 + 2|\lambda_0| \Delta t \leq e^{2|\lambda_0| \Delta t}.$$

□

Remark 5.2. In the case where $|\lambda_0| \Delta t \leq c_0$ with constant $c_0 \in (0, 2)$, the constant c in Theorem 5.1 can be replaced by $c = (1 - c_0/2)^{-1}$.

For the MCS scheme, we have the following positive stability result.

Theorem 5.3. Let $c = \max\{1/\theta, 2\}$. For the scheme (4.5) there holds:

(a) If $\theta \geq \frac{1}{3}$, then $|R(z_0, z_1, z_2, w_0)^n| \leq e^{c|\lambda_0|t_n}$ whenever $z_0, z_1, z_2 \in \mathbb{R}$ satisfy (5.12),

(b) If $\frac{1}{2} \leq \theta \leq 1$, then $|R(z_0, z_1, z_2, w_0)^n| \leq e^{c|\lambda_0|t_n}$ whenever $z_0, z_1, z_2 \in \mathbb{C}$ satisfy (5.12).

Proof. It suffices again to consider $n = 1$. Define

$$P = R(z_0, z_1, z_2, 0) \quad \text{and} \quad Q = \frac{1}{p} + \frac{z_0}{p^2} + (1 - \theta) \frac{z_1 + z_2}{p^2}.$$

It is easily verified that

$$R(z_0, z_1, z_2, w_0) = P + w_0 Q + \frac{1}{2} \frac{w_0^2}{p^2}.$$

By [23, Sect. 2.1] we immediately have that the condition (5.12) implies

$$\left| 1 + \frac{w}{p} \right| \leq \left| 1 - \frac{1}{2\theta} \right| + \frac{1}{2\theta}.$$

Next, it is readily seen that $|p| \geq 1$ and $|p| \geq \theta|z_1 + z_2|$. Hence,

$$|Q| \leq \left| 1 + \frac{z_0}{p} + (1 - \theta) \frac{z_1 + z_2}{p} \right| \leq \left| 1 + \frac{w}{p} \right| + \theta \left| \frac{z_1 + z_2}{p} \right| \leq \left| 1 - \frac{1}{2\theta} \right| + \frac{1}{2\theta} + 1 = c.$$

Consequently, if $|P| \leq 1$, then we obtain

$$|R(z_0, z_1, z_2, w_0)| \leq 1 + c|\lambda_0| \Delta t + \frac{1}{2}(|\lambda_0| \Delta t)^2 \leq e^{c|\lambda_0| \Delta t}.$$

Parts (a) and (b) now directly follow by invoking [24, Thm. 2.5] and [20, Thm. 2.7], respectively, which provide sufficient conditions for $|P| \leq 1$ under (5.12). □

In a similar fashion, the subsequent stability result has been obtained in [22, Thm. 3.7] for the MCS2 scheme.

Theorem 5.4. *Let $c = \max\{1/\theta, 2\}$. For the scheme (4.6) there holds:*

- (a) *If $\theta \geq \frac{1}{3}$, then $\|C(z_0, z_1, z_2, w_0)^n\| \leq e^{2c|\lambda_0|t_n}$ whenever $z_0, z_1, z_2 \in \mathbb{R}$ satisfy (5.12),*
- (b) *If $\frac{1}{2} \leq \theta \leq 1$, then $\|C(z_0, z_1, z_2, w_0)^n\| \leq e^{2c|\lambda_0|t_n}$ whenever $z_0, z_1, z_2 \in \mathbb{C}$ satisfy (5.12).*

In Theorems 5.3 and 5.4 above, the parts (a) and (b) are relevant to, respectively, diffusion-dominated and convection-dominated equations.

Remark 5.5. *In [30, Thm. 3.3] it has been proved that for any given $\theta \in [\frac{1}{4}, \frac{1}{2}]$ there exists a value $\gamma \in [\frac{1}{2}, 1)$ such that $|R(z_0, z_1, z_2, 0)| \leq 1$ for all complex numbers z_0, z_1, z_2 satisfying the natural condition*

$$|z_0| \leq 2\gamma\sqrt{\Re z_1 \Re z_2}, \quad \Re z_1 \leq 0, \quad \Re z_2 \leq 0. \quad (5.13)$$

The quantity γ can be viewed as a bound on the relative size of the mixed derivative coefficient, that is, on $|\rho|$. For the pertinent γ , the stability bounds in Theorems 5.3 and 5.4 for the schemes (4.5) and (4.6) also hold whenever $z_0, z_1, z_2 \in \mathbb{C}$ satisfy (5.13). In the special case $\theta = \frac{1}{3}$ the result from [30] yields that $\gamma \geq (2 + \sqrt{10})/6 \approx 0.86$ and it has been conjectured in [20] that the optimal value $\gamma \approx 0.96$. Hence, in this case, (5.13) forms only a slightly stronger condition than (5.12).

For the SC2A scheme (4.7), deriving a stability bound of the kind in Theorems 5.1(d) and 5.4 is more complicated, among others due to the fact that the implicit method for the PDE part is a not a one-step but a two-step method. We shall leave this topic for future research. We mention, however, that for (4.7) the positive result has been obtained in [14, Thm. 4.2] that if $\theta \geq \frac{2}{3}$, then for any given $z_0, z_1, z_2 \in \mathbb{R}$ satisfying (5.12) the pertinent matrix $C(z_0, z_1, z_2, 0)$ is power-bounded.

The stability results relevant to the scalar test equation (5.1) can directly be employed in a stability analysis of the splitting schemes for two-dimensional PIDEs with constant convection and diffusion coefficients and with the integral term representing a two-dimensional cross-correlation (or convolution). It is well-known that the transformation to the log-price variable $x_i = \ln(s_i)$ (for $i = 1, 2$) turns (2.1) with general probability density function f into such a PIDE, where the spatial domain is \mathbb{R}^2 . The obtained probability density function in our case is that of the double exponential distribution. Semidiscretization on a uniform Cartesian grid on the whole \mathbb{R}^2 domain with second-order central finite differences for convection and diffusion and a standard discretization (employing bilinear interpolation as in Subsection 3.2) of the double integral then yields a linear system of ODEs with doubly infinite matrix (operator) A that is of block Laurent type. Its constituent matrices $A^{(M)}$, A_1 , A_2 , $A^{(J)}$ are also of this type, and stability can be analyzed in the l_2 -norm by means of a Fourier transform, cf. [26, Sect. 3.4]. In particular, the (scaled) eigenvalues of these matrices, which are given through their symbols, are readily seen to satisfy (5.12) and $|\lambda_0| \leq \lambda$. Consequently, the stability theorems of this section can be used to arrive at positive, unconditional stability results for the operator splitting schemes of Section 4 when applied to the PIDE for the log-price variable. For the sake of brevity, we shall omit the details here.

Additional, complementary stability results relevant to (one- and two-dimensional) PIDEs have been derived in [6] for the scheme (4.2), in [32] for the scheme (4.4) and in [22] for the schemes (4.5) and (4.6).

6 Numerical study

In this section we present ample numerical experiments for the seven operator splitting schemes formulated in Section 4, which provides important insight in their convergence behavior and mutual performance. For the CNFI scheme (4.2) we choose $l = 2$ iterations, as noted in Section 4. The experiments involve three different parameter sets for the two-asset Kou model, labelled as 1, 2, and 3. The parameter set 1 is taken from Clift & Forsyth [6]. Set 2 is a blend of parameters

considered for the one-asset Kou model by Almendral & Oosterlee [1] and d’Halluin, Forsyth & Vetzal [9] (see also Toivanen [36]). Set 3 has been newly constructed and includes a relatively large value for the product λT , i.e., the expected number of jumps in $[0, T]$. For the truncated spatial domain, we (heuristically) select $S_{\max} = 20K, 10K, 30K$ for sets 1, 2, 3, respectively.

Table 3

Parameter sets for the two-asset Kou jump-diffusion model.

	σ_1	σ_2	r	ρ	λ	p_1	p_2	η_{p_1}	η_{q_1}	η_{p_2}	η_{q_2}	K	T
Set 1	0.12	0.15	0.05	0.30	0.50	0.40	0.60	1/0.20	1/0.15	1/0.18	1/0.14	100	1
Set 2	0.15	0.20	0.05	0.50	0.20	0.3445	0.50	3.0465	3.0775	3	2	100	0.2
Set 3	0.20	0.30	0.05	0.70	8	0.60	0.65	5	4	4	3	100	1

6.1 Option values and numerical convergence behavior

Figure 3 shows the numerically computed³ option value surfaces for the European put-on-the-average option and the three parameter sets from Table 3 on the asset price domain $[0, 3K] \times [0, 3K]$ and $t = T$.

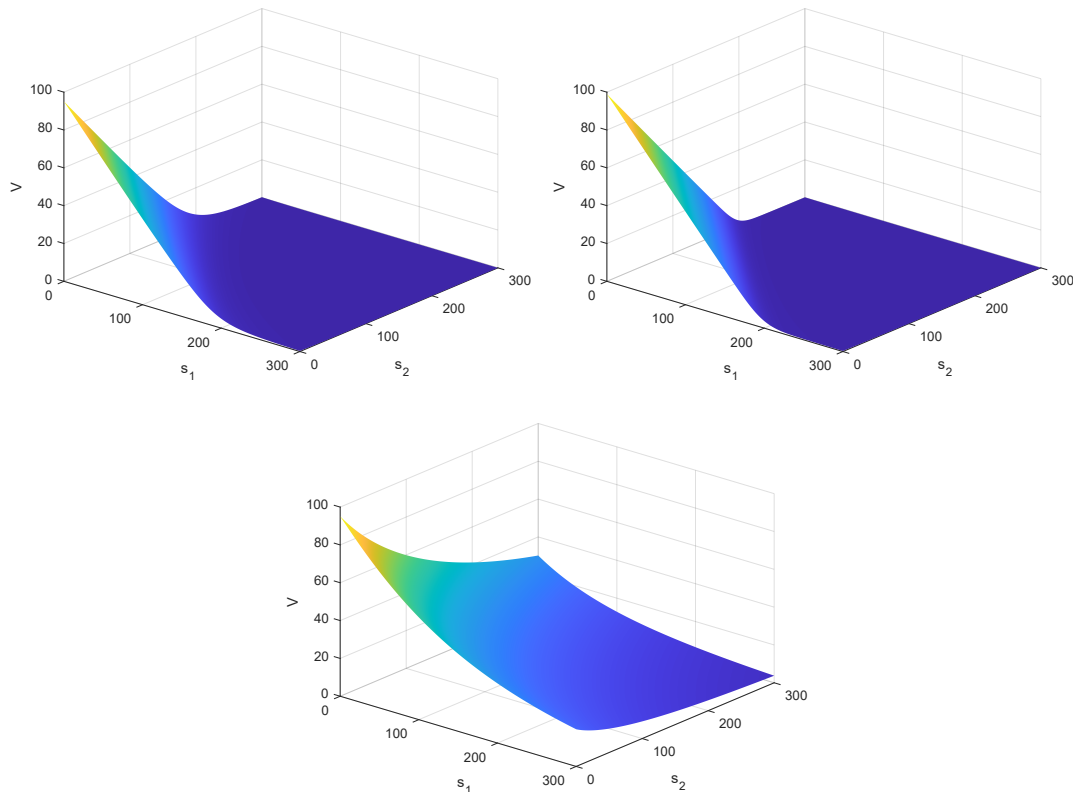


Figure 3: Option value surfaces for the European put-on-the-average option under the two-asset Kou model in the case of parameter set 1 (top left), 2 (top right) and 3 (bottom) given in Table 3.

For future reference, accurate approximations to the option values have been computed⁴ for specifically chosen spot prices $S_0^{(1)}, S_0^{(2)}$ of the two assets in a neighborhood of the strike K , see Table 4.

³Using $m_1 = m_2 = 200$, $N = 100$ and the MCS2 scheme.

⁴Using $m_1 = m_2 = 1000$, $N = 500$ and the MCS2 scheme with spline interpolation.

Table 4

European put-on-the-average option value approximations for parameter sets 1, 2 and 3.

Set 1			
	$S_0^{(1)} = 90$	$S_0^{(1)} = 100$	$S_0^{(1)} = 110$
$S_0^{(2)} = 90$	8.9385	6.0316	3.8757
$S_0^{(2)} = 100$	5.9655	3.8038	2.3370
$S_0^{(2)} = 110$	3.7641	2.2978	1.3771

Set 2			
	$S_0^{(1)} = 90$	$S_0^{(1)} = 100$	$S_0^{(1)} = 110$
$S_0^{(2)} = 90$	9.6863	5.5616	2.6400
$S_0^{(2)} = 100$	5.6162	2.6929	1.1264
$S_0^{(2)} = 110$	2.7570	1.1670	0.5246

Set 3			
	$S_0^{(1)} = 90$	$S_0^{(1)} = 100$	$S_0^{(1)} = 110$
$S_0^{(2)} = 90$	32.7459	31.0984	29.5758
$S_0^{(2)} = 100$	30.5796	29.0181	27.5770
$S_0^{(2)} = 110$	28.5830	27.1033	25.7396

We next examine, through numerical experiments, the convergence behavior of the seven operator splitting schemes formulated in Section 4 for the temporal discretization of the semidiscrete two-dimensional Kou PIDE. Take $m_1 = m_2 = m$. Consider a region of financial interest

$$\text{ROI} = \{(s_1, s_2) : \frac{1}{2}K < s_1, s_2 < \frac{3}{2}K\}$$

and define the *temporal discretization error* on this ROI for $t = T$ by

$$\hat{E}^{\text{ROI}}(m, N) = \max \left\{ |V_{i,j}(T) - V_{i,j}^{N'}| : \Delta t = T/N' \text{ and } (s_{1,i}, s_{2,j}) \in \text{ROI} \right\}. \quad (6.1)$$

Clearly, this error is measured in the (important) maximum norm. The MCS2 scheme is applied with 3000 time steps to obtain a reference value for the exact semidiscrete solution $V(T)$ to (3.9). For each of the seven operator splitting schemes formulated in Section 4, we study the temporal discretization error for a sequence of values N , where the approximation $V^{N'}$ to $V(T)$ is computed using N' time steps. Here N' is chosen in function of N depending on the specific scheme, so as to arrive at a fair comparison between the ADI schemes and between the IMEX schemes.

For the three ADI schemes we find in our experiments that the evaluation of the two-dimensional integral part, by means of the algorithm from Subsection 3.2, takes the same computational time as the solution of four to six pertinent tridiagonal linear systems (using an a priori *LU* factorization). The scheme (4.5) employs two evaluations of the integral part, whereas (4.6) and (4.7) each use only one such evaluation. Next, both schemes (4.5) and (4.6) require the solution of four tridiagonal systems, whereas (4.7) contains only two tridiagonal systems. Accordingly, for a fair mutual comparison, we apply the ADI schemes (4.5), (4.6) and (4.7) with, respectively, $N' = N$, $N' = \lfloor 3N/2 \rfloor$ and $N' = 2N$ time steps.

For the four IMEX schemes, a proper choice of N' depends on the method used for solving the pertinent linear systems involving the matrix $I - \frac{1}{2}\Delta t A^{(D)}$. Recall that this matrix is sparse,

but has a large bandwidth. Hence, due to fill-in, the direct solution of these linear systems by LU factorization becomes prohibitively expensive when m gets large. Below we shall consider CPU times in the case of the BiCGSTAB iterative method. It turns out that in this case a sound comparison is achieved by applying the two schemes (4.1) and (4.4) with $N' = 2N$ time steps, the scheme (4.3) with $N' = \lceil 3N/2 \rceil$ time steps, and the scheme (4.2) with just $N' = N$ time steps. Notice that in the latter scheme (with $l = 2$) two linear systems arise per time step, whereas in each of the other three IMEX schemes it is only one.

For each of the seven splitting schemes, the temporal discretization errors $\widehat{E}^{\text{ROI}}(m, N)$ have been computed for $m = 200$ and a sequence of values N between 10 and 1000. Here a direct solver for the linear systems has been used also in the case of the four IMEX schemes, to ensure that the approximation errors due to the iterative solver do not affect the outcome. Figure 4 displays the obtained temporal errors for all three parameter sets given in Table 3, where the left column shows the results for the IMEX schemes and the right column the results for the ADI schemes.

From Figure 4 we observe the positive result that, for each given scheme and parameter set, the temporal errors are bounded from above by a moderate value and decrease monotonically as N increases. As expected, the CNFE scheme (4.1) shows an order of convergence equal to one, whereas all other six splitting schemes reveal a desirable order of convergence equal to two. By repeating the numerical experiments for spatial grids that are finer (e.g. $m = 300, 400, 500$) or coarser (e.g. $m = 50, 100$) we obtain results that are visually identical to those displayed in Figure 4. This indicates that, for each splitting scheme, the temporal errors are essentially independent of the spatial grid size, and hence, its observed convergence order is valid in a stiff sense, which is very favorable.

It is interesting to remark that the error constants become larger as the intensity of the jumps increases, keeping all else fixed. This has been observed in additional numerical experiments for increasing values of λ between 0 and 10.

As already alluded to above, we give CPU times in the case where the BiCGSTAB method⁵ is employed for the iterative solution of the pertinent linear systems in the four IMEX schemes. Here an ILU preconditioner is used, which has been computed upfront. As a natural starting vector for the iteration we have taken V^{n-1} for the schemes (4.1), (4.3), (4.4) and Y_{k-1} for the scheme (4.2). The tolerance⁶ $\text{tol} = 1\text{e-}10$ is heuristically chosen small enough so that the approximation error due to the iterative solution of the linear systems in each time step does not appear to strongly affect the temporal convergence behavior of the IMEX schemes, as considered in Figure 4.

Table 5 shows the obtained individual CPU times (in seconds) for the seven operator splitting schemes, applied with N' time steps, in the numerical solution of the two-dimensional Kou PIDE (2.1) for parameter set 1 and a range of values $m_1 = m_2 = m$ between 100 and 1000 with $N = m/2$. The algorithm of Subsection 3.2 has been employed to approximate the integral (3.2).

A perusal of the results of Table 5 indicates that, for each splitting method, the CPU time is essentially directly proportional to Nm^2 , which is as desired. Clearly, for each given m , the obtained CPU times for the CNFE, CNFI and CNAB schemes (using N' time steps) are almost identical and for the IETR scheme it is either equal to this or somewhat larger. Next, for each given m , the CPU times for the MCS, MCS2 and SC2A schemes are almost the same and about half of those obtained for the IMEX schemes.

Among the four IMEX schemes, the CNAB scheme yields the smallest error constants in our numerical experiments, cf. Figure 4. Among the three ADI schemes, the MCS2 scheme has the smallest error constant in all our experiments. Overall, the MCS2 scheme is preferred. It yields temporal errors that are smaller than or approximately equal to those of the CNAB scheme, but is computationally significantly faster. Also, the linear systems in each time step of the MCS2 scheme are just tridiagonal, and can therefore be solved exactly in a highly efficient manner.

⁵As implemented in Matlab version R2020b through the function `bicgstab`.

⁶For the relative residual error in the 2-norm.

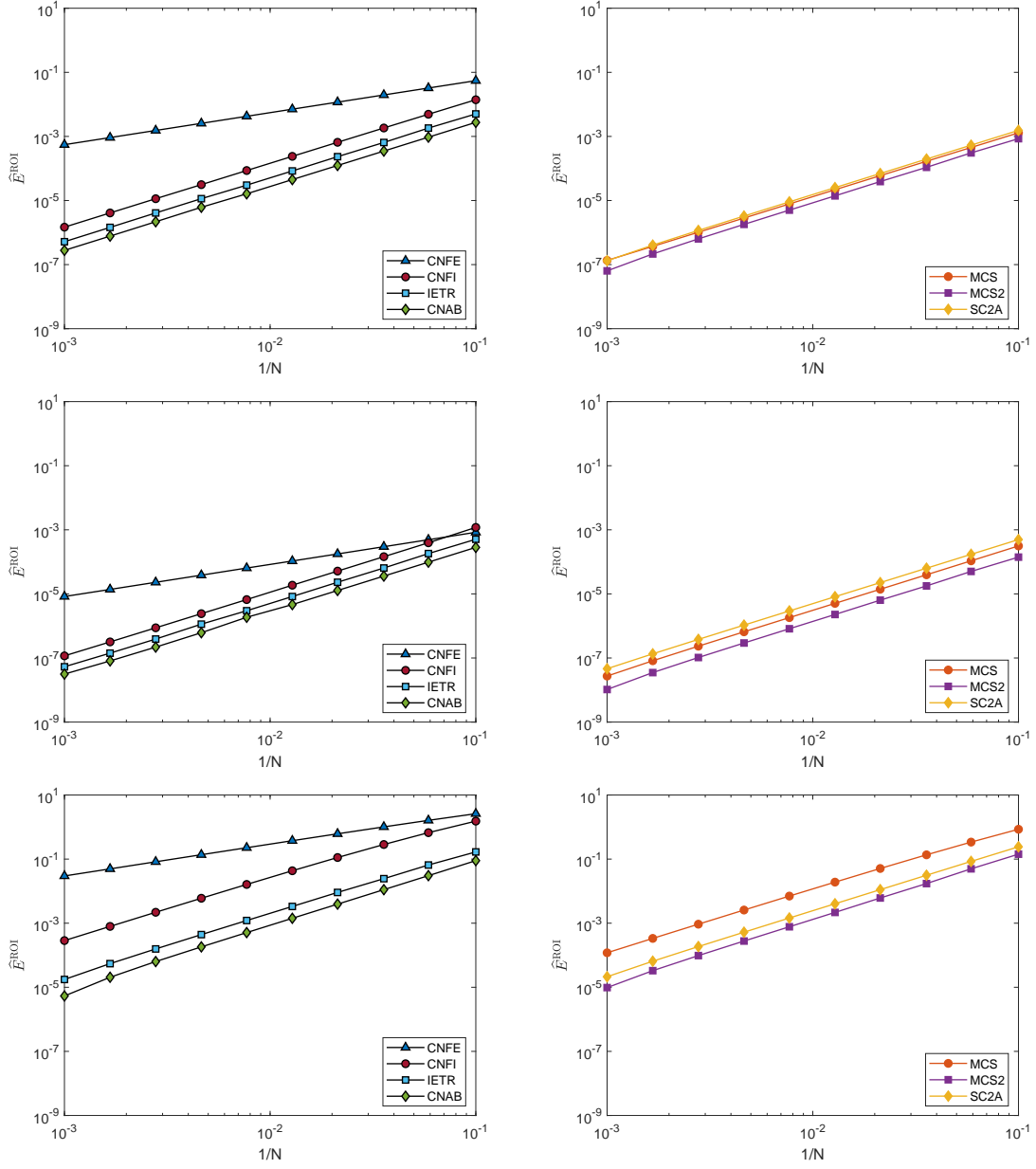


Figure 4: Temporal errors $\hat{E}^{\text{ROI}}(200, N)$ of the seven operator splitting schemes under consideration. IMEX schemes on the left side and ADI schemes on the right side, with parameter set 1 (top), set 2 (middle) and set 3 (bottom) from Table 3. The CNFI and MCS schemes are applied with step size $\Delta t = T/N$, the IETR and MCS2 schemes are applied with $\Delta t = T/[3N/2]$ and the CNFE, CNAB, SC2A schemes are applied with $\Delta t = T/(2N)$.

Table 5

CPU times (s) for the seven operator splitting schemes applied with N' time steps (given between brackets) in the numerical solution of (2.1) for parameter set 1 with $m_1 = m_2 = m$ and $N = m/2$.

m	N	CNFE ($2N$)	CNFI (N)	IETR ($3N/2$)	CNAB ($2N$)	MCS (N)	MCS2 ($3N/2$)	SC2A ($2N$)
100	50	0.4	0.4	0.4	0.4	0.2	0.2	0.2
200	100	2.3	2.0	2.1	2.3	1.1	1.1	1.1
300	150	8.8	8.5	8.8	9.0	4.4	4.4	4.3
400	200	23.8	24.1	25.4	24.6	13.6	13.5	14.0
500	250	49.1	49.2	56.8	49.2	27.0	27.0	28.4
1000	500	503.2	499.7	555.2	501.0	247.0	240.6	253.3

6.2 The Greeks

The Greeks are mathematical derivatives of the option value with respect to underlying variables and parameters. They constitute a measure for risk that indicates how sensitive an option value is to changes in underlying variables and parameters and are crucial for hedging strategies. In this subsection we consider the numerical approximation of the Delta and Gamma Greeks. Delta is a measure for the rate of change of the option value with respect to a change in an underlying asset price. As there are two underlying assets, there are two Deltas:

$$\Delta_1 = \frac{\partial v}{\partial s_1} \quad \text{and} \quad \Delta_2 = \frac{\partial v}{\partial s_2}.$$

Next, Gamma measures the rate of change of a Delta with respect to a change in an underlying asset price. There are three different Gammas:

$$\Gamma_{11} = \frac{\partial \Delta_1}{\partial s_1} = \frac{\partial^2 v}{\partial s_1^2}, \quad \Gamma_{22} = \frac{\partial \Delta_2}{\partial s_2} = \frac{\partial^2 v}{\partial s_2^2} \quad \text{and} \quad \Gamma_{12} = \frac{\partial \Delta_1}{\partial s_2} = \frac{\partial^2 v}{\partial s_2 \partial s_1} = \frac{\partial \Delta_2}{\partial s_1} = \Gamma_{21}.$$

By virtue of the finite difference discretization that has been defined in Section 3, the Delta and Gamma Greeks can directly be approximated, at essentially no computational cost, by applying the second-order central finite difference formulas considered in Subsection 3.1 to the option value approximations on the spatial grid.

As an illustration, Figure 5 displays the numerically⁷ obtained Delta and Gamma surfaces at maturity for the European put-on-the-average option under the two-asset Kou model for parameter set 1. As expected, the Delta surfaces are steepest around the line segment $s_1 + s_2 = 2K$ and, correspondingly, the Gamma surfaces are highest there.

Similarly to the option value, we study the temporal convergence behavior of all operator splitting schemes in the case of the five Greeks. Akin to (6.1), the temporal discretization error in the case of Delta Δ_k ($k = 1, 2$) is defined by

$$\widehat{E}_{\Delta_k}^{\text{ROI}}(m, N) = \max \left\{ |(\Delta_k)_{i,j}(T) - (\Delta_k)_{i,j}^{N'}| : \Delta t = T/N' \quad \text{and} \quad (s_{1,i}, s_{2,j}) \in \text{ROI} \right\}. \quad (6.2)$$

Here $\Delta_k(T)$ denotes the pertinent finite difference matrix for convection applied to the reference value for the exact semidiscrete solution $V(T)$ given in Subsection 6.1. Next, $\Delta_k^{N'}$ is equal to the same finite difference matrix applied to the approximation $V^{N'}$ of $V(T)$ that is generated by any one of the seven operator splitting schemes. Analogous temporal discretization error definitions hold in the case of $\Gamma_{11}, \Gamma_{22}, \Gamma_{12}$.

Figure 6 displays the temporal errors in the case of the five Greeks and parameter set 1 for $m = 200$ and the same sequence of values N between 10 and 1000 as before. We arrive at the same conclusions on the temporal convergence behavior of the seven splitting schemes as obtained

⁷Using $m_1 = m_2 = 200$, $N = 100$ and the MCS2 scheme.

in Subsection 6.1 regarding the option value. In particular, besides CNFE, all splitting schemes reveal a stiff order of convergence equal to two, and MCS2 has the best performance among all these schemes.

We note that the somewhat larger errors that are observed for the CNFI, IETR, CNAB schemes when N is small are attributed to the nonsmoothness of the initial (payoff) function and could be alleviated by applying four (instead of two) half time steps with IMEX Euler at the start of the time stepping, cf. Section 4.

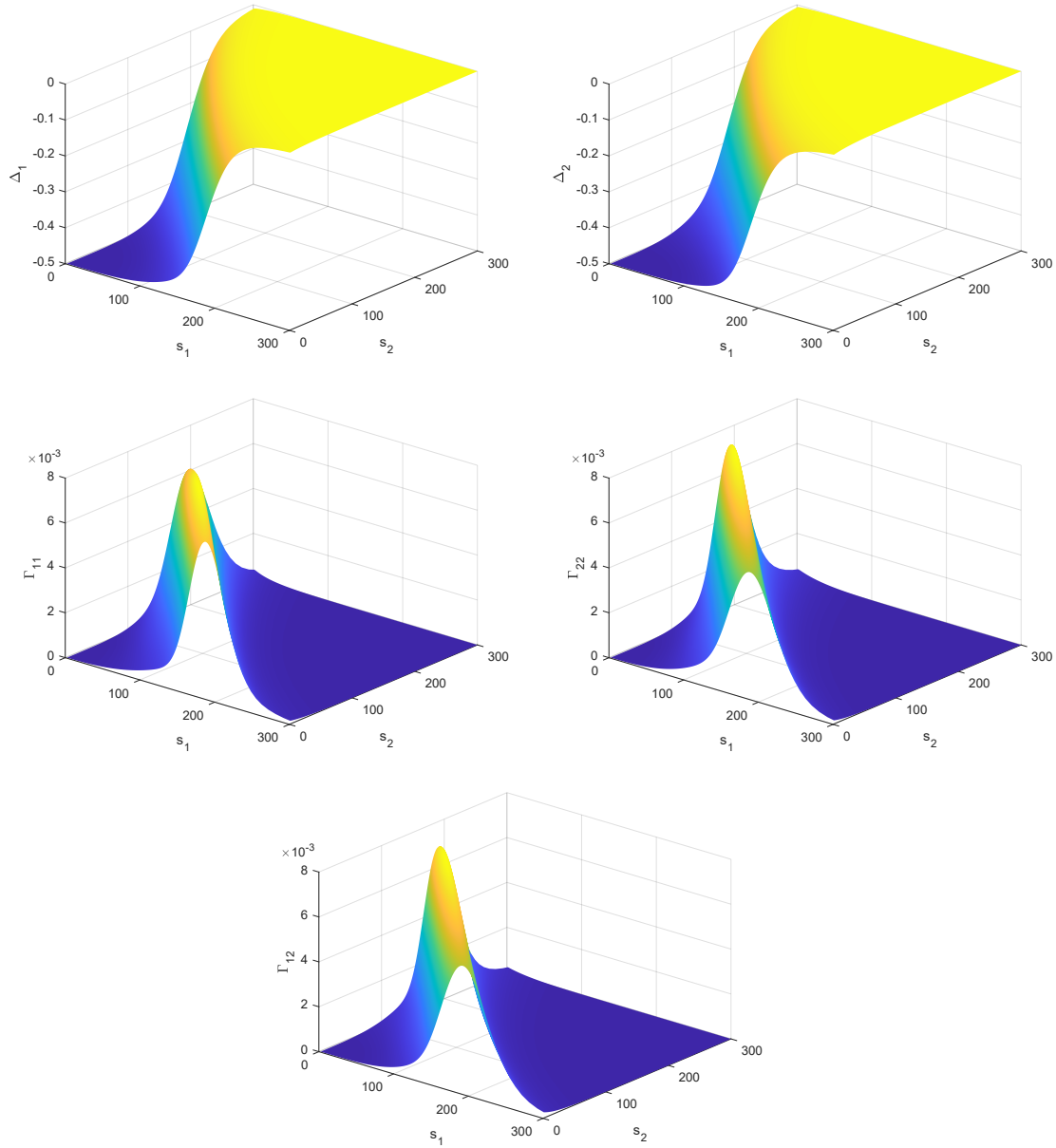


Figure 5: First-order Greeks Δ_1 (top left) and Δ_2 (top right) and second-order Greeks Γ_{11} (middle left), Γ_{22} (middle right) and Γ_{12} (bottom) for the European put-on-the-average option under the two-asset Kou model in the case of parameter set 1.

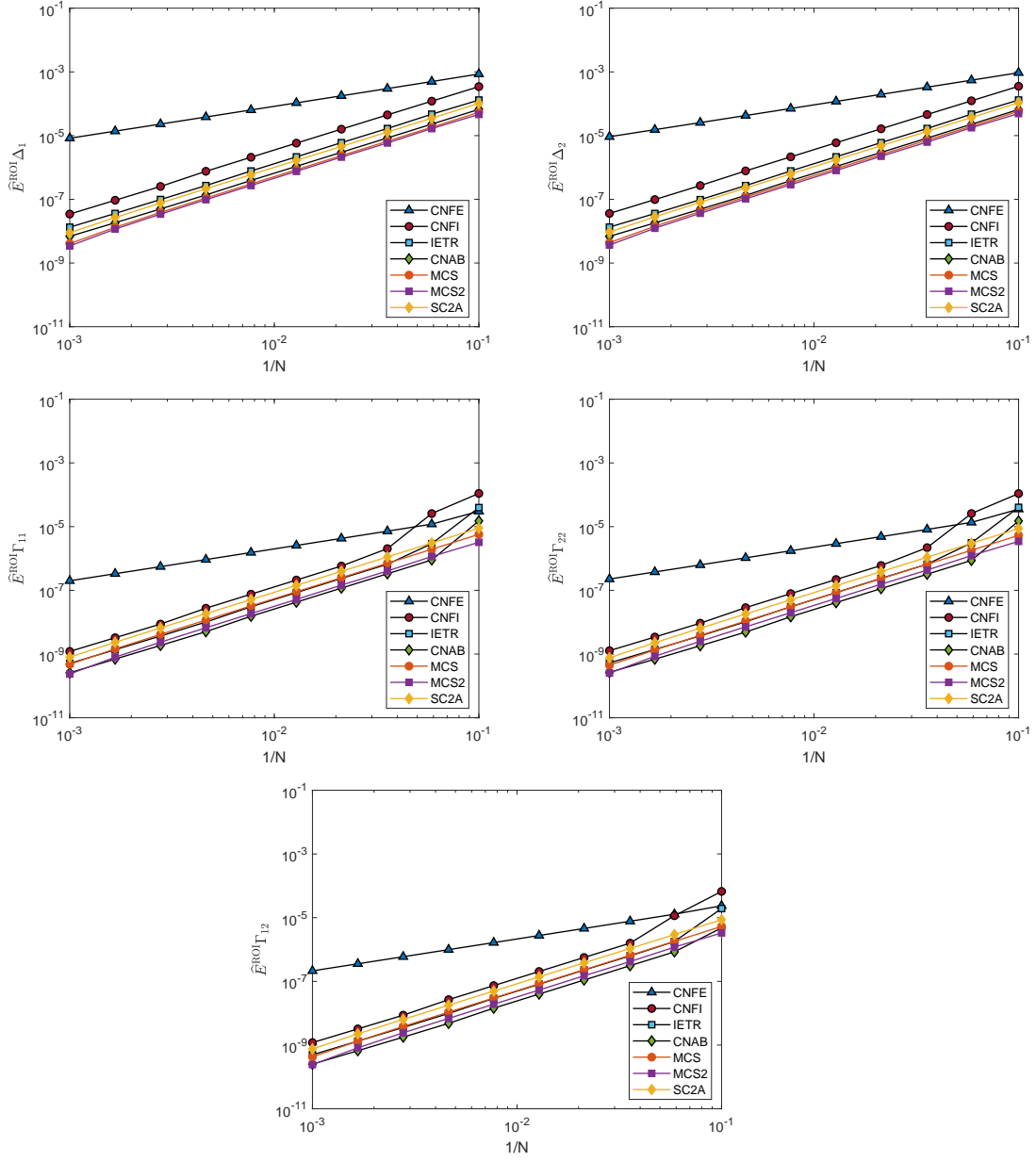


Figure 6: Temporal errors of the seven operator splitting schemes under consideration in the case of the five Greeks and parameter set 1: $\widehat{E}_{\Delta_1}^{\text{ROI}}$ (top left), $\widehat{E}_{\Delta_2}^{\text{ROI}}$ (top right), $\widehat{E}_{\Gamma_{11}}^{\text{ROI}}$ (middle left), $\widehat{E}_{\Gamma_{22}}^{\text{ROI}}$ (middle right) and $\widehat{E}_{\Gamma_{12}}^{\text{ROI}}$ (bottom). The CNFI and MCS schemes are applied with step size $\Delta t = T/N$, the IETR and MCS2 schemes are applied with $\Delta t = T/[3N/2]$ and the CNFE, CNAB, SC2A schemes are applied with $\Delta t = T/(2N)$.

7 Conclusions

We have studied the valuation of European options under the two-asset Kou jump-diffusion model via the numerical solution of the pertinent two-dimensional time-dependent PIDE. A first main contribution of our paper is the extension of an algorithm derived by Toivanen [36], which enables a highly efficient numerical evaluation of the nonlocal double integral appearing in this PIDE. The computational cost of the acquired algorithm is optimal: it is directly proportional to the

number of grid points in the spatial discretization. Also, it is simple to implement and requires little memory usage. Subsequently, for the efficient discretization in time of the semidiscretized two-dimensional Kou PIDE, we have investigated seven modern operator splitting schemes of the IMEX and the ADI kind. Every splitting scheme conveniently treats the integral term in an explicit fashion. Through rigorous analysis and extensive numerical experiments, we have examined the stability and convergence behavior, respectively, of the splitting schemes as well as their relative performance. All of the considered schemes, except for the first-order CNFE scheme, show a desirable, stiff order of temporal convergence equal to two. The MCS2 scheme, successively developed by in 't Hout & Welfert [24] for PDEs and in 't Hout & Toivanen [22] for PIDEs, stood out favorably among the splitting schemes in view of its superior efficiency. This conclusion agrees with the results recently obtained by Boen & in 't Hout [4] in the case of the two-dimensional Merton PIDE.

All schemes and results in our present paper can straightforwardly be extended to the case of a two-asset jump-diffusion model that has a mixture of independent and perfectly correlated jumps with log-double-exponential distributions, leading to a sum of three integrals in the two-dimensional PIDE, which is handled as a single (integral) term in the IMEX and ADI schemes, cf. also Kaushansky, Lipton & Reisinger [26] in a different context.

For the valuation of American-style options under a given two-asset jump-diffusion model, a two-dimensional partial integro-differential complementarity problem (PIDCP) is obtained. The adaptation of the operator splitting schemes of our present paper to such problems has recently been studied in Boen & in 't Hout [3] in the case of the two-asset Merton model. Here, for their effective adaptation, the combination with an iterated version of the Ikonen–Toivanen (IT) splitting technique [16, 17, 36] has been considered as well as the penalty approach [6, 11, 37]. Notably, the MCS2-IT(2) method [3], which denotes the combination of the MCS2 scheme with two iterations of IT splitting, is found to be an efficient and stable temporal discretization method for the two-dimensional Merton PIDCP. We expect that the same conclusion will hold in the case of the two-dimensional Kou PIDCP.

For PIDEs or PIDCPs that stem from infinite activity processes, such as the VG, NIG and CGMY models, the development and analysis of operator splitting methods is still largely open in the literature and this forms an aim for future research. Here a useful idea is to replace the small jumps, that is, the jumps with sizes not exceeding a given small positive threshold ε , by a scaled Brownian motion, see [7, 8].

Declaration of interest

The authors report no conflicts of interest. The authors alone are responsible for the content and writing of the paper.

Acknowledgements

The authors wish to thank the two anonymous reviewers for their various useful comments and suggestions, which have led to a substantial improvement of the original version of this paper.

References

- [1] A. Almendral and C. W. Oosterlee. Numerical valuation of options with jumps in the underlying. *Appl. Numer. Math.*, 53:1–18, 2005.
- [2] L. Andersen and J. Andreasen. Jump-diffusion processes: volatility smile fitting and numerical methods for option pricing. *Rev. Deriv. Res.*, 4:231–262, 2000.
- [3] L. Boen and K. J. in 't Hout. Operator splitting schemes for American options under the two-asset Merton jump-diffusion model. *Appl. Numer. Math.*, 153:114–131, 2020.

- [4] L. Boen and K. J. in 't Hout. Operator splitting schemes for the two-asset Merton jump-diffusion model. *J. Comp. Appl. Math.*, 387:112309, 2021.
- [5] M. Briani, R. Natalini, and G. Russo. Implicit-explicit numerical schemes for jump-diffusion processes. *Calcolo*, 44:33–57, 2007.
- [6] S. S. Clift and P. A. Forsyth. Numerical solution of two asset jump diffusion models for option valuation. *Appl. Numer. Math.*, 58:743–782, 2008.
- [7] R. Cont and P. Tankov. *Financial modelling with Jump Processes*. Chapman & Hall/CRC Financial Mathematics Series. CRC Press, 2004.
- [8] R. Cont and E. Voltchkova. A finite difference scheme for option pricing in jump diffusion and exponential Lévy models. *SIAM J. Numer. Anal.*, 43:1596–1626, 2005.
- [9] Y. d'Halluin, P. A. Forsyth, and K. R. Vetzal. Robust numerical methods for contingent claims under jump diffusion processes. *IMA J. Numer. Anal.*, 25:87–112, 2005.
- [10] L. Feng and V. Linetsky. Pricing options in jump-diffusion models: an extrapolation approach. *Oper. Res.*, 56:304–325, 2008.
- [11] P. A. Forsyth and K. R. Vetzal. Quadratic convergence for valuing American options using a penalty method. *SIAM J. Sci. Comp.*, 23:2095–2122, 2002.
- [12] J. Frank, W. Hundsdorfer, and J. G. Verwer. On the stability of implicit-explicit linear multistep methods. *Appl. Numer. Math.*, 25:193–205, 1997.
- [13] A. Ghosh and C. Mishra. Highly efficient parallel algorithms for solving the Bates PIDE for pricing options on a GPU. *Appl. Math. Comp.*, 409:126411, 2021.
- [14] W. Hundsdorfer and K. J. in 't Hout. On multistep stabilizing correction splitting methods with applications to the Heston model. *SIAM J. Sci. Comp.*, 40:A1408–A1429, 2018.
- [15] W. Hundsdorfer and J. G. Verwer. *Numerical Solution of Time-Dependent Advection-Diffusion-Reaction Equations*. Springer, 2003.
- [16] S. Ikonen and J. Toivanen. Operator splitting methods for American option pricing. *Appl. Math. Lett.*, 17:809–814, 2004.
- [17] S. Ikonen and J. Toivanen. Operator splitting methods for pricing American options under stochastic volatility. *Numer. Math.*, 113:299–324, 2009.
- [18] K. J. in 't Hout. On the contractivity of implicit-explicit linear multistep methods. *Appl. Numer. Math.*, 42:201–212, 2002.
- [19] K. J. in 't Hout. *Numerical Partial Differential Equations in Finance Explained*. Palgrave Macmillan, 2017.
- [20] K. J. in 't Hout and C. Mishra. Stability of the modified Craig–Sneyd scheme for two-dimensional convection-diffusion equations with mixed derivative term. *Math. Comp. Simul.*, 81:2540–2548, 2011.
- [21] K. J. in 't Hout and J. Toivanen. Application of operator splitting methods in finance. In *Splitting Methods in Communication, Imaging, Science, and Engineering*, pages 541–575. Springer, 2016.
- [22] K. J. in 't Hout and J. Toivanen. ADI schemes for valuing European options under the Bates model. *Appl. Numer. Math.*, 130:143–156, 2018.
- [23] K. J. in 't Hout and B. D. Welfert. Stability of ADI schemes applied to convection-diffusion equations with mixed derivative terms. *Appl. Numer. Math.*, 57(1):19–35, 2007.

- [24] K. J. in 't Hout and B. D. Welfert. Unconditional stability of second-order ADI schemes applied to multi-dimensional diffusion equations with mixed derivative terms. *Appl. Numer. Math.*, 59:677–692, 2009.
- [25] K. J. in 't Hout and M. Wyns. Convergence of the Modified Craig–Sneyd scheme for two-dimensional convection-diffusion equations with mixed derivative term. *J. Comp. Appl. Math.*, 296:170–180, 2016.
- [26] V. Kaushansky, A. Lipton, and C. Reisinger. Numerical analysis of an extended structural default model with mutual liabilities and jump risk. *J. Comp. Sci.*, 24:218–231, 2018.
- [27] S. G. Kou. A jump-diffusion model for option pricing. *Manag. Sci.*, 48:1086–1101, 2002.
- [28] Y. Kwon and Y. Lee. A second-order finite difference method for option pricing under jump-diffusion models. *SIAM J. Numer. Anal.*, 49:2598–2617, 2011.
- [29] R. C. Merton. Option pricing when underlying stock returns are discontinuous. *J. Finan. Econ.*, 3:125–144, 1976.
- [30] C. Mishra. A new stability result for the modified Craig–Sneyd scheme applied to two-dimensional convection-diffusion equations with mixed derivatives. *Appl. Math. Comp.*, 285:41–50, 2016.
- [31] R. Rannacher. Finite element solution of diffusion problems with irregular data. *Numer. Math.*, 43:309–327, 1984.
- [32] S. Salmi and J. Toivanen. IMEX schemes for pricing options under jump-diffusion models. *Appl. Numer. Math.*, 84:33–45, 2014.
- [33] S. Salmi, J. Toivanen, and L. von Sydow. An IMEX-scheme for pricing options under stochastic volatility models with jumps. *SIAM J. Sci. Comp.*, 36:B817–B834, 2014.
- [34] W. Schoutens. *Lévy Processes in Finance: Pricing Financial Derivatives*. Wiley, 2003.
- [35] D. Tavella and C. Randall. *Pricing Financial Instruments: The Finite Difference Method*. Wiley, 2000.
- [36] J. Toivanen. Numerical valuation of European and American options under Kou’s jump-diffusion model. *SIAM J. Sci. Comp.*, 30:1949–1970, 2008.
- [37] R. Zvan, P. A. Forsyth, and K. R. Vetzal. Penalty methods for American options with stochastic volatility. *J. Comp. Appl. Math.*, 91:199–218, 1998.